

1 ***Pseudomonas aeruginosa* can diversify after host cell invasion to establish**
2 **multiple intracellular niches**

3
4 Naren G. Kumar^{a, #}, Vincent Nieto^{a, #}, Abby R. Kroken^{a, †}, Eric Jedel^a, Melinda R. Grosser^{a, ††}, Mary
5 E. Hallsten^a, Matteo M. E. Mettrucio^a, Timothy L. Yahr^b, David J. Evans^{a, c}, and Suzanne M. J.
6 Fleiszig^{a, d*}

7
8 a. Herbert Wertheim School of Optometry & Vision Science, University of California, Berkeley,
9 CA USA
10 b. Department of Microbiology and Immunology, University of Iowa, IA USA
11 c. College of Pharmacy, Touro University California, Vallejo, CA USA
12 d. Graduate Groups in Vision Science, Microbiology, and Infectious Diseases & Immunity,
13 University of California, Berkeley, CA USA

14
15 Running title: Intracellular *P. aeruginosa* diversification and antibiotic tolerance

16
17 # Contributed equally to the first authorship

18
19 Current addresses: † Dept. of Microbiology and Immunology, Loyola University Chicago,
20 Maywood, IL, USA, †† Dept. of Biology, University of North Carolina, Asheville, NC USA

21
22 * Corresponding author. School of Optometry, University of California, Berkeley, CA 94720-
23 2020, USA. Tel. 1 (510) 643-0990, Fax. 1 (510) 643-5109. Email: fleiszig@berkeley.edu

24 **Abstract**

25

26 Within epithelial cells, *Pseudomonas aeruginosa* depends on its type three secretion system
27 (T3SS) to escape vacuoles and replicate rapidly in the cytosol. Previously, it was assumed that
28 intracellular subpopulations remaining T3SS-negative (and therefore in vacuoles) were destined
29 for degradation in lysosomes, supported by data showing vacuole acidification. Here, we report in
30 both corneal and bronchial human epithelial cells that vacuole associated-bacteria can persist,
31 sometimes in the same cells as cytosolic bacteria. Using a combination of phase-contrast, confocal,
32 and correlative light and electron microscopy, we also found they can demonstrate biofilm-
33 associated markers: *cdrA* and cyclic-di-GMP (c-di-GMP). Vacuolar-associated bacteria, but not
34 cytosolic counterparts, tolerated the cell-permeable antibiotic ofloxacin. Surprisingly, use of
35 mutants showed that both persistence in vacuoles and ofloxacin tolerance were independent of the
36 biofilm-associated protein CdrA or exopolysaccharides (Psl, Pel, alginate). A T3SS mutant
37 (Δ *exsA*) unable to escape vacuoles phenocopied vacuolar-associated sub-populations in wild-type
38 PAO1-infected cells, results revealing that epithelial cell death depended upon bacterial viability.
39 Intra-vital confocal imaging of infected mouse corneas confirmed that *P. aeruginosa* formed
40 similar intracellular sub-populations within epithelial cells *in vivo*. Together, these results show
41 that *P. aeruginosa* differs from other pathogens by diversifying intracellularly into vacuolar and
42 cytosolic sub-populations that both contribute to pathogenesis. Their different gene expression and
43 behavior (e.g., rapid replication versus slow replication/persistence) suggest cooperation favoring
44 both short- and long- term interests and another potential pathway to treatment failure. How this
45 intracellular diversification relates to previously described “acute versus chronic” virulence gene-
46 expression phenotypes of *P. aeruginosa* remains to be determined.

47 **Importance**

48

49 *Pseudomonas aeruginosa* can cause sight- and life-threatening opportunistic infections, and its
50 evolving antibiotic resistance is a growing concern. Most *P. aeruginosa* strains can invade host
51 cells, presenting a challenge to therapies that do not penetrate host cell membranes. Previously,
52 we showed that the *P. aeruginosa* type III secretion system (T3SS) plays a pivotal role in survival
53 within epithelial cells, allowing escape from vacuoles, rapid replication in the cytoplasm, and
54 suppression of host cell death. Here, we report the discovery of a novel T3SS-negative sub-
55 population of intracellular *P. aeruginosa* within epithelial cells that persist in vacuoles rather than
56 the cytoplasm, and that tolerate a cell-permeable antibiotic (ofloxacin) that is able to kill cytosolic
57 bacteria. Classical biofilm-associated markers, although demonstrated by this sub-population, are
58 not required for vacuolar persistence or antibiotic tolerance. These findings advance our
59 understanding of how *P. aeruginosa* hijacks host cells, showing it diversifies into multiple
60 populations with T3SS-negative members enabling persistence whilst rapid replication is
61 accomplished by more vulnerable T3SS-positive siblings. Intracellular *P. aeruginosa* persisting
62 and tolerating antibiotics independently of the T3SS or biofilm-associated factors could present
63 additional challenges to development of more effective therapeutics.

64

65

66

67

68

69

70 **INTRODUCTION**

71

72 *Pseudomonas aeruginosa* is a significant cause of morbidity and mortality including burn-wound
73 infections, septicemia, catheter-associated infections, corneal infections, community-acquired and
74 nosocomial pneumonia, and chronic lung disease in persons with cystic fibrosis (CF). *P.*
75 *aeruginosa* infections are notoriously difficult to treat due to a combination of inherent
76 antimicrobial resistance and the versatility and adaptability of this opportunistic pathogen (1–5).

77 While often considered an extracellular pathogen, several decades of work across many research
78 labs have established that clinical isolates of *P. aeruginosa* can internalize and survive in host
79 cells, including in animal models of infection (6–14). Despite this, surprisingly little is known
80 about the intracellular lifestyle of *P. aeruginosa*, and many questions remain about how it
81 contributes to disease pathogenesis and recalcitrance to therapeutics.

82 Previously, we showed that *P. aeruginosa* survival inside cells is modulated by the type three
83 secretion system (T3SS) and several of its effectors (ExoS, ExoT and ExoY), with ExoS playing
84 a prominent role (11, 15, 16). While the RhoGAP activity of ExoS (and ExoT) can counter
85 bacterial internalization by host cells via antiphagocytic activity (15, 17–20), bistability results in
86 a lack of T3SS expression in many extracellular bacteria, effectively tempering antiphagocytic
87 activity and allowing some population members to invade cells (11, 16, 21). Once inside the cell,
88 efficient T3SS triggering allows expression of the T3SS, which in an ExoS-dependent manner
89 inhibits vacuole acidification, enables escape from the endocytic vacuole, inhibits autophagy, and
90 allows rapid replication of bacteria in the host cytosol (10, 17, 22, 23). Differing from other
91 intracellular bacteria that use host cytoskeletal components for intracellular motility (24), *P.*
92 *aeruginosa* then utilizes its own pili/twitching motility to disseminate throughout the host cell (25).

93 Meanwhile, ExoS further supports intracellular survival by delaying lytic host cell death
94 effectively preserving the intracellular niche (16), and it drives formation of plasma membrane
95 blebs to which some bacteria traffic and replicate within (9, 19). These blebs can subsequently
96 disconnect from cells, becoming vesicles with intact membranes that can carry enclosed
97 live/swimming bacteria to distant sites (9). Mutations affecting T3SS needle assembly, T3SS toxin
98 secretion, or expression of the entire T3SS ($\Delta exsA$), restrict intracellular bacteria to endocytic
99 vacuoles (10, 11, 15), which we previously presumed were destined for degradation within
100 lysosomes (10).

101 In a previous study, we showed that mutants defective in twitching motility, and therefore
102 unable to disseminate intracellularly, formed non-motile bacterial aggregates inside host cells
103 surrounded by electron-lucid halos on electron micrographs (25). This led us to explore if *P.*
104 *aeruginosa* was able to produce biofilm-associated factors inside infected host cells.

105 Biofilm formation has long been recognized as a strategy that bacteria use to survive under
106 adverse environmental conditions including during infections (26, 27). In human infections, *P.*
107 *aeruginosa* biofilm formation can be associated with chronic persistence in the host, through a
108 combination of phenotypic and genotypic adaptations that allow acquisition of essential nutrients
109 and confer resistance to antimicrobial therapies and host defenses (28–31). Investigations of *P.*
110 *aeruginosa* biofilm architecture and composition have revealed the presence multiple bacterial
111 exopolysaccharides in the biofilm matrix including Psl, Pel and alginate, the latter most prominent
112 in *P. aeruginosa* biofilms in CF (32, 33). CdrA is a bacterial protein with production regulated by
113 the bacterial second messenger c-di-GMP that reinforces and protects the biofilm matrix (34, 35).
114 Extracellular DNA (eDNA) is another major component of the biofilm matrix that interacts with
115 polysaccharide components and can modulate bacterial dispersal (36–38).

116 To test the hypothesis that intracellular *P. aeruginosa* could demonstrate biofilm-associated
117 markers we used gene expression reporters for *cdrA* encoding the biofilm-matrix protein and c-di-
118 GMP (which triggers biofilm formation). Results for both corneal and bronchial epithelial cells
119 showed distinct intracellular populations when cells were infected with wild-type *P. aeruginosa*,
120 with *cdrA*-expressing bacteria localized to vacuoles and T3SS-expressing bacteria in the cytosol,
121 often in the same cell. The data also showed potentially important functional differences between
122 the two populations, with cytosolic *P. aeruginosa* sensitive to the cell permeable antibiotic
123 ofloxacin, and vacuolar populations demonstrating ofloxacin tolerance even at high
124 concentrations. Surprisingly, neither persistence in vacuoles nor ofloxacin tolerance required *cdrA*
125 or any of the three exopolysaccharides (*alg*, *psl*, *pel*) known to be associated with biofilm
126 formation. Raising potentially interesting implications for the impact of antibiotics on infection
127 pathogenesis, the results also showed that the vacuolar-located antibiotic survivors were able to
128 trigger cell death.

129 The discovery that *P. aeruginosa* can establish niches in multiple locations within the same
130 epithelial cells (cytoplasm, membrane blebs, vacuoles) differs from other bacterial pathogens
131 which traffic to either vacuoles or the cytoplasm in a linear fashion. The finding that the bacteria
132 in these alternate locations express different survival/virulence determinants and vary in antibiotic
133 susceptibility predicts a “covering of the bases” for the overall population. Interestingly, this
134 pattern of gene expression occurring simultaneously in infected cells is reminiscent of the “acute”
135 versus “chronic” infection expression phenotypes, which are generally thought to represent
136 entirely different infection types. How intracellular diversification relates to those previously
137 described infection phenotypes, and the relevance of these results to antibiotic treatment failure *in*
138 *vivo*, will require further investigation.

139

140 **RESULTS**

141

142 **Bacteria expressing biofilm-associated factors *cdrA*, c-di-GMP localize to vacuoles in human**

143 **epithelial cells.** To determine if biofilm-associated factors were expressed by intracellular *P.*

144 *aeruginosa*, human corneal and bronchial epithelial cells were imaged 6 h after inoculation with

145 *P. aeruginosa* that report expression of *cdrA* (pMG078) or c-di-GMP (pFY4535) (39, 40) (Table

146 1). Results were compared to bacteria that instead report T3SS expression (10, 11). Following a 3

147 h infection period to allow bacteria to invade cells, extracellular bacteria were eliminated using the

148 non-cell permeable antibiotic amikacin, thereby allowing intracellular bacteria to be selectively

149 visualized (8, 10, 11).

150 Aligning with our previously published data (9–11, 16), T3SS-expressing intracellular bacteria

151 localized to the cytosol in both epithelial cell types, wherein they replicated rapidly and

152 disseminated throughout the cytoplasm (Fig. 1). Bacteria expressing the biofilm-associated factors

153 *cdrA*- or c-di-GMP-were also detected among the intracellular population. Rather than being in

154 the cytosol, this sub-population appeared to be contained in vacuolar-like niches that remained

155 stable over time (Fig. 1A). To confirm that *cdrA*-GFP reporting bacteria (pseudo-colored red) were

156 within vacuoles as opposed to being in aggregates within the cytosol, real-time phase-contrast

157 microscopy was used to visualize the cellular compartment in which they were contained. Fig. 1B

158 shows *cdrA*-GFP reporting PAO1F (11, 16, 21) located in vacuoles in corneal epithelial cells and

159 Fig. 1C shows the same PAO1F phenotype in bronchial epithelial cells. A different wild-type

160 parental strain PAO1P (35, 41) (see Table 1) also showed the same *cdrA*-GFP reporting vacuolar-

161 located phenotype within corneal epithelial cells (data not shown). Thus, for two PAO1 parental

162 wild-types, some of the sub-population expressing *cdrA* were found restricted within membrane-
163 bound circular phase-clear regions implicating vacuoles and distinguishing them from possible
164 intracellular cytosolic aggregates.

165 Having shown distinct intracellular phenotypes of *P. aeruginosa*, the percentage of corneal
166 epithelial cells containing *cdrA*-expressing intracellular bacteria was then quantified. Cells were
167 infected with PAO1F expressing the *cdrA*-GFP reporter (pMG078) and total intracellular bacteria
168 detected with an anti-*Pseudomonas* antibody at 6 h post-infection (Fig. 1D). The percentage of
169 cells containing intracellular bacteria that expressed only *cdrA* (*cdrA*^{on}) was quantified, along with
170 the percentage of cells containing intracellular bacteria not expressing *cdrA* (*cdrA*^{off}), or those
171 containing both. Of 520 cells analyzed, 7.7 % contained only *cdrA*-expressing bacteria (red bar),
172 and 9.6 % contained *cdrA*^{off} bacteria (green bar), while 6 % contained both phenotypes (yellow
173 bar) (Fig. 1D). Images below quantitative data show examples of each of these different categories.

174 To determine if a lack of vacuolar escape into the cytosol necessarily leads to *cdrA* expression,
175 we performed the same analysis using a mutant lacking ExsA, the transcriptional activator of the
176 T3SS (PAO1F Δ exsA) (9). This mutant does not express the T3SS and remains in vacuoles because
177 the T3SS is required for vacuolar escape and survival in the cytosol (10). Results (Fig. 1E)
178 confirmed that at this time point (6 h post-infection), *exsA*-mutants were only present in vacuoles
179 and that the percentage of cells containing internalized bacteria was similar to wild-type parent
180 PAO1F (see Fig. 1D). Importantly, the distribution of *cdrA*^{on} versus *cdrA*^{off} bacteria found in
181 vacuoles for *exsA*-mutant infected cells (Fig. 1E) was similar to wild-type-infected cells (see Fig
182 1D). Images of *cdrA*^{on} and *cdrA*^{off} categories for *exsA*-mutant infected cells are shown (Fig. 1E).

183 Thus, both wild-type bacteria and T3SS (*exsA*) mutants can express *cdrA* when in vacuoles,
184 and this occurs in a similar percentage of the infected host cell population under these experimental

185 conditions.

186

187 **Vacuolar localization does not require *cdrA*.** C-di-GMP is a trigger for biofilm formation while
188 CdrA is the only known biofilm matrix protein made by *P. aeruginosa*. Since *cdrA* was expressed
189 only in bacteria localized to vacuoles, we next asked if vacuolar localization depends on CdrA,
190 and potentially also on biofilm formation. Thus, we compared a *cdrA* mutant (PAO1P Δ *cdrA*) to
191 wild-type (PAO1P) for the ability to persist in vacuoles. First, we confirmed that the *cdrA* mutant
192 did not differ from wild-type in its ability to invade corneal epithelial cells (Fig. 2A) and did not
193 have a different impact on cell viability over time (data not shown). Next, we compared the
194 percentage of corneal epithelial cells that contained at least one *cdrA*-GFP expressing bacterium
195 after infection with wild-type (PAO1P) or *cdrA* mutant (PAO1P Δ *cdrA*) at 6 h post-infection.
196 Results showed that the *cdrA* mutant and wild-type trafficked to vacuoles in a similar percentage
197 of cells over the 6 h period (Fig. 2B). Phase-contrast microscopy also showed that mutants unable
198 to express *cdrA* (Δ *cdrA*) trafficked to vacuoles at 6 h post-infection (Fig. 2C). This further shows
199 that vacuolar persistence at 6 h post-infection did not require CdrA (Fig. 2B and C).

200

201 **Among intracellular bacteria, the *cdrA*-expressing population is more tolerant to ofloxacin
202 than the T3SS-expressing population.** Biofilm-associated bacteria tend to be more antibiotic
203 tolerant. Thus, we next explored if the intracellular *cdrA*-expressing population could better resist
204 an antibiotic than their cytosolic T3SS-expressing cell-mates. This was done using ofloxacin, an
205 antibiotic differing from amikacin (in part) by being able to penetrate host cell membranes. Wild-
206 type bacteria were allowed to internalize for 3 h, before exposing epithelial cells to either amikacin
207 alone (non-cell permeable, kills only extracellular bacteria) or amikacin plus ofloxacin (to

208 additionally target intracellular bacteria). Ofloxacin concentrations were chosen according to the
209 MIC for the PAO1 strain variants used (see methods). For PAO1F, the MIC for ofloxacin was
210 determined to be 0.25 μ g/mL, and for that reason concentrations used ranged from 0.25 - 4 μ g/mL
211 (1X- 16X MIC). Fig. 3 shows time-lapse imaging of intracellular *P. aeruginosa* gene expression
212 using T3SS-GFP and *cdrA*-GFP reporters, and the percentage of epithelial cells containing at least
213 one GFP-positive bacterial cell at 6 and 12 h post-infection.

214 Cytosolic T3SS^{on} populations showed significant susceptibility to ofloxacin at 1 μ g/mL (4X
215 MIC) at both 6 h and 12 h, with fewer infected cells detected over time (Fig. 3A, B, C and
216 Supplemental Video S1). In contrast, intracellular *cdrA*^{on} bacteria continued to report with
217 ofloxacin treatment concentrations all the way up to 4 μ g/mL (16X MIC) at both 6 and 12 h post-
218 infection with ~ 4-6 % of epithelial cells containing *cdrA*^{on} bacteria (Fig. 3D, E, F and
219 Supplemental Video S2). These results showed that vacuolar *cdrA*-expressing bacteria were better
220 able to resist killing by ofloxacin than T3SS-reporting cytosolic bacteria in the same infected host
221 cell population.

222

223 **Correlative light and electron microscopy confirmed viability and vacuolar localization of**
224 **ofloxacin tolerant *P. aeruginosa*.** Since the fluorescent signal from intracellular bacteria may
225 persist long after bacterial cell death (42) and *cdrA* expression is induced upon cell contact,
226 correlative light and electron microscopy (CLEM) was used to confirm that *cdrA*-GFP reporting
227 bacteria surviving above MIC concentrations of ofloxacin were both intracellular and localized to
228 vacuoles. CLEM is essentially a combination of wide-field immunofluorescence and electron
229 microscopy (EM) using the same section to localize fluorescence with morphological details (e.g.
230 of a cell) (43, 44). Ofloxacin was used at 6 h post-infection (with PAO1F) at a concentration that

231 can clear the cytosolic population (1 μ g/mL, see Fig. 3A). Fig. 4 shows three individual cells
232 containing *cdrA*-GFP expressing bacteria in vacuoles, all localized to the perinuclear region where
233 late endosomes are expected to reside, each containing ~1 - 4 bacterial cells. Since vacuolar-
234 localized bacteria have intact cell walls after antibiotic treatment, it suggests that vacuolar-
235 localized populations are viable. This outcome supports the conclusion from our wide-field
236 fluorescence and DIC/phase-contrast microscopy experiments (Fig. 1A, B; Fig. 2C; Fig. 3D), that
237 ofloxacin tolerant *cdrA*-expressing sub-populations can be intracellular *P. aeruginosa* and that
238 they localize to vacuoles.

239

240 **Detectable *cdrA* expression does not correlate with ofloxacin resistance.** While the experiments
241 above show that *cdrA*-expressing intracellular bacteria localized to vacuoles, not all vacuolar-
242 located bacteria expressed *cdrA*. Heterogeneity among vacuolar bacteria is not surprising, as they
243 likely transition through various phenotypes after internalization/replication and as maturation of
244 the vacuole alters their environment. Here, we sought to explore ofloxacin susceptibility among
245 all vacuolar bacteria in a wild-type infection, not just those expressing *cdrA*. To specifically label
246 (all intracellular bacteria) and study the effect of ofloxacin on the total population of intracellular
247 bacteria, ofloxacin was used to kill the susceptible population in cells infected with wild-type
248 bacteria expressing an arabinose-inducible reporter (pGFP_{arabinose}; see Methods & Supplemental
249 Fig. S1) where only the survivors express GFP. Epithelial cells containing at least one ofloxacin
250 survivor were then quantified at 6 and 12 h (Fig. 5). As expected, when ofloxacin was not used or
251 used only at sub-lethal concentrations (< MIC 0.50 μ g/mL), epithelial cells infected with wild-
252 type bacteria were found to contain both cytosolic and vacuolar-localized bacteria (Fig. 5A). When
253 ofloxacin was used 2X above the MIC (0.5 μ g/mL) or higher, there was a gradual reduction in the

254 number of cytosolic bacteria while only vacuolar populations continued to persist (Fig. 5A). The
255 percentage of cells containing vacuoles with ofloxacin tolerant bacteria was similar at 6 h (Fig.
256 5B) and 12 h (Fig. 5C), showing stability during the intervening time. Comparison to percentage
257 of cells containing any ofloxacin survivors in vacuoles to those containing only *cdrA*^{on} survivors
258 (~10 %, Fig. 5B and C versus ~4 %, Fig. 3E and F) suggested additional ofloxacin tolerant bacteria
259 (in vacuoles) besides those expressing *cdrA* (Fig. 5A versus 3D). These results suggested that
260 while vacuolar bacteria can express *cdrA* and can also tolerate high doses of ofloxacin, while
261 expression of *cdrA* is dispensable for vacuolar localization and tolerating high concentrations of
262 the antibiotic (Fig 2C). Unfortunately, experiments to test this more directly could not be done
263 using bacteria simultaneously expressing both reporters (i.e., arabinose-inducible GFP and *cdrA*)
264 because expression of dual fluorescent reporters in *P. aeruginosa* impairs bacterial fitness and
265 affects the invasion of host cells. Instead, we used isogenic *cdrA* mutants as discussed below.

266

267 **CdrA and biofilm-associated EPS is dispensable for ofloxacin resistance of vacuolar *P.***
268 ***aeruginosa*.** Having shown expression of the biofilm-associated gene *cdrA* in a subset of vacuolar
269 bacteria, along with vacuolar bacteria as being more tolerant to ofloxacin than cytosolic bacteria,
270 and that ofloxacin tolerant bacteria could express *cdrA*, we next explored if CdrA was required for
271 ofloxacin resistance of vacuolar bacteria. To more broadly study the contribution of biofilm
272 formation, we also considered biofilm-associated exopolysaccharides (EPS). Thus, mutants in
273 CdrA ($\Delta cdrA$), exopolysaccharides (ΔEPS ; *psl*, *pel*, and alginate) or both ($\Delta cdrA/\Delta EPS$) were
274 tested for intracellular ofloxacin resistance using time-lapse imaging as described above. Since the
275 *in vitro* MIC of PAO1P (the wild-type parent of these mutants) was 4 μ g/mL versus 0.25 μ g/mL
276 for PAO1F (used above) the ofloxacin concentration was adjusted accordingly from 0 - 64 μ g/mL

277 (0 – 16X MIC). Fig. 6 A-D shows the percentage of corneal epithelial cells containing at least one
278 GFP-expressing bacterial cell at 12 h post-infection. Use of $pGFP_{\text{arabinose}}$ detected all viable
279 intracellular *P. aeruginosa*, while *cdrA*-GFP specifically reported biofilm-associated sub-
280 populations. Surprisingly, there was no significant difference between wild-type and *cdrA* mutants
281 in the number of cells still containing viable intracellular bacteria after ofloxacin treatment at all
282 concentrations up to 64 $\mu\text{g}/\text{mL}$ (16X MIC) (Fig. 6A and B) with each strain entering ~15-20 % of
283 the corneal epithelial cells (Fig. 6A and B, grey bars) and *cdrA*-GFP expressing vacuolar sub-
284 populations in ~5-10 % of those cells (Fig. 6A and B, red bars). This was shown using arabinose-
285 inducible GFP to detect all intracellular ofloxacin survivors, and the *cdrA*-reporter to detect only
286 the subset reporting *cdrA* promotor activity (which still occurs in *cdrA* mutants) (Fig. 6B). Thus,
287 *cdrA* is not required for the ofloxacin resistance exhibited by vacuolar *P. aeruginosa* in addition
288 to not being required for vacuolar localization.

289 As shown in Figures 6 C and D, similar results were obtained for the ΔEPS triple mutant
290 lacking all three biofilm associated exopolysaccharides (EPS), and a quadruple mutant additionally
291 lacking CdrA ($\Delta EPS/\Delta cdrA$ mutant). In each case the percentage of epithelial cells containing
292 *cdrA*-promotor expressing vacuolar sub-populations at each ofloxacin concentration was similar.

293 Control experiments confirmed that PAO1F and PAO1P showed similar levels of
294 internalization into human corneal epithelial cells at 4 h post-infection, as did PAO1P relative to
295 its *cdrA* and *EPS* mutants (Supplemental Fig. S2).

296

297 **T3SS mutants unable to exit vacuoles show similar ofloxacin resistance to vacuolar located**
298 **wild-type PAO1.** The above data suggested that something about vacuolar localization might
299 promote ofloxacin resistance, independently of expression of classical biofilm-associated factors

300 (e.g. CdrA and EPS) that co-incidentally occur in that location, possibly even a physical feature of
301 the vacuole itself rather than a bacterial-driven mechanism. As a first step toward understanding
302 this, we used a T3SS mutant (PAO1F Δ exsA) unable to escape the vacuoles (9–11, 17). Fig. 7
303 shows time-lapse imaging of human corneal epithelial cells infected with PAO1F Δ exsA expressing
304 pGFP_{arabinose} to visualize all intracellular bacteria over time with and without ofloxacin and
305 subsequently quantify percentage of cells containing internalized bacteria. As expected, the Δ exsA
306 mutant localized only to vacuoles observed as GFP-expressing puncta within the epithelial cells
307 that increased in fluorescence over time (Fig. 7A). This population survived exposure to ofloxacin
308 at 6 and 12 h post-infection (Fig. 7B, Supplemental Video S3). CLEM was then used to ensure
309 that persistent vacuolar populations were due to live bacteria not residual GFP signal from dead
310 bacteria (42). Results showed the Δ exsA mutant localized to perinuclear vacuoles with multiple
311 bacteria in a single membrane-bound compartment (Fig. 7C, inset). Some of these vacuolar
312 bacteria were seen surviving exposure to ofloxacin (1 μ g/mL) as shown by bacteria maintaining
313 their cell wall integrity in perinuclear vacuoles (Fig. 7D, inset). Thus, T3SS mutants of *P.*
314 *aeruginosa* that cannot escape vacuoles can phenocopy the T3SS-off subpopulation of wild-type
315 when infecting corneal epithelial cells with respect to tolerating ofloxacin, supporting the
316 possibility that vacuolar localization itself enables survival.

317

318 **Vacuolar-localized *P. aeruginosa* can drive host cell death.** The above experiments showed that
319 vacuolar bacteria can be more tolerant to ofloxacin. To further explore the significance of the
320 vacuolar phenotype, we next examined how it impacts the host cell. Using the same experimental
321 protocols as above, the kinetics of human corneal epithelial cell death during infection were
322 measured using propidium iodide. After cells were infected with PAO1 Δ exsA (occupies only

323 vacuoles) for 3 h, extracellular bacteria were killed using amikacin (200 μ g/mL), then ofloxacin 0
324 - 4 μ g/mL (0 -16X MIC) was added into the media to also kill the cytosolic population. Cells
325 containing intracellular bacteria showed increasing cell death from 4 - 24 h up to maximum of ~
326 40 % of the total population, the kinetics not significantly affected by ofloxacin exposure up to 4
327 μ g/mL (16X MIC) (Fig. 8A). A significant reduction in cell death was only observed when the
328 ofloxacin concentration was increased to 25 μ g/mL (100X MIC). While 25 μ g/mL (100X MIC)
329 of ofloxacin did not reduce visible GFP-expressing (pGFP_{arabinose}) (Fig. 8B), the effect on cell death
330 suggests supraphysiological concentrations of antibiotic are required to inactivate vacuolar-
331 localized populations. This further suggests an active role of intracellular vacuolar bacteria in the
332 outcome of host cell death.

333

334 **Diversification of intracellular phenotypes also occurs during *in vivo* corneal infection.** It has
335 been three decades since we initially reported that *P. aeruginosa* can invade corneal epithelial cells
336 *in vivo* in mice, including the first observation that they could be in membrane-bound vacuoles as
337 shown using transmission electron microscopy (TEM) (6). Because TEM required sample fixation,
338 it was unclear if these bacteria were destined to be degraded, to enter the cytoplasm, or to persist
339 in the vacuoles.

340 More recently, we used intravital confocal/2-photon imaging without fixation to confirm *in*
341 *vivo* that when *P. aeruginosa* enters the cell cytosol it can colonize the cytoplasm or can traffic to
342 membrane blebs (45). Since the present study revealed intracellular diversification leading to
343 cytosolic and vacuolar bacteria coexisting in the same infected cell population *in vitro*, we next
344 asked if this could also occur *in vivo*. To explore this, we used a murine scarification model that
345 enables *P. aeruginosa* to colonize the epithelium. This was done using Lyz2cre+/mRosa-DTR

346 mice that constitutively express a red fluorescent protein in their cell membranes with along with
347 green/yellow myeloid-derived cells and infecting these mice with mPAO1 constitutively
348 expressing blue-fluorescent protein (pMG055). In this way, we were able to study the localization
349 of infecting bacteria relative to the host cell membranes and differentiate myeloid and non-myeloid
350 derived cell types in the cornea. Live confocal imaging at 15 h post-infection showed three
351 intracellular phenotypes similar in appearance to our *in vitro* observations. These included both
352 cytoplasmic and membrane bleb-contained *P. aeruginosa*, in addition to intracellular aggregates
353 appearing to be vacuoles containing bacteria.

354 The absence of tissue fixation/sectioning allowed us to additionally collect temporal data in
355 3D in intact eyes during infection. Doing so, we were able to observe *in vivo* multiple phenomena
356 that we have reported when *P. aeruginosa* infects cultured corneal and other epithelial cells. This
357 included a sub-population in the cytosol demonstrating twitching motility, a second sub-population
358 demonstrating swimming motility inside plasma membrane blebs, and a third population stationary
359 and appearing to be confined to vacuoles (Fig. 9, Supplemental Videos S4, S5, S6). These results
360 suggest that all of the intracellular phenomena that we have reported when *P. aeruginosa* infects
361 cultured cells occur during infection *in vivo*.

362

363 DISCUSSION

364

365 Bacteria surviving inside host cells generally orchestrate their localization and replication via
366 secretion of virulence factors to establish a niche in either the cytosol or in subcellular membrane-
367 bound compartments such as vacuoles, secretory vesicles, and endoplasmic reticulum (46–49).
368 Previously, we showed that when *P. aeruginosa* invades epithelial cells it can utilize its type 3

369 secretion system (T3SS) to escape vacuoles (17). This is followed by rapid replication and
370 dissemination throughout the cytosol, with the T3SS effector ExoS used to avoid autophagy and
371 to construct and occupy host cell plasma membrane blebs (9, 11, 19). We have also reported that
372 *P. aeruginosa* differs from other pathogens by not depending on host cell cytoskeletal elements
373 for intracellular motility, with bacteria instead using their own appendages (25). This includes
374 pilus-driven twitching motility in the cytoplasm and flagella-mediated swimming motility within
375 membrane blebs (11).

376 The T3SS of *P. aeruginosa* is expressed by only some population members even under
377 inducing conditions (11, 50). Since the T3SS is required for vacuolar escape but not cell entry,
378 T3SS-off subpopulation members remain in vacuoles after being internalized (9–11). Our prior
379 model was that these were destined for degradation in lysosomes, an idea supported by vacuole
380 acidification (10). Here, we instead found that T3SS-off *P. aeruginosa* remained viable over long
381 periods of time in vacuoles, shown using both corneal and bronchial epithelial cells. We also found
382 they could differentiate into a phenotype expressing biofilm-associated factors that are not
383 expressed by their cytoplasmic counterparts. These vacuolar T3SS-off bacteria were often present
384 in cells also containing cytosolic T3SS-on bacteria. Thus, we have identified a novel (third)
385 intracellular niche for *P. aeruginosa* inside epithelial cells in which the bacteria are in a different
386 phenotypic state (T3SS-off, biofilm-producing, non-motile) in addition to being in a different
387 intracellular location (vacuoles). Use of CLEM to simultaneously study the fine structure of the
388 host cells versus location of CdrA-expressing bacteria confirmed that this biofilm protein was
389 expressed by intracellular bacteria residing in vacuoles.

390 The significance of *P. aeruginosa* residing in epithelial cell vacuoles could potentially have
391 multiple impacts on disease outcome, including presenting challenges to therapeutics. Firstly, we

392 found vacuolar bound bacteria were more tolerant to a cell permeable antibiotic than their cytosolic
393 counterparts. Persistence and antibiotic recalcitrance of vacuole-contained bacteria could be a
394 contributor to why *P. aeruginosa* infections are difficult to treat, and why infection can rebound
395 after antibiotic treatment is ended. Secondly, the data showed the vacuolar population triggered
396 lytic host cell death contingent on their viability, even when the cytosolic population is eliminated
397 using an antibiotic. Indeed, use of an antibiotic at concentrations killing only the cytosolic
398 population actually *promotes* this type of cell death because the cytosolic population uses ExoS to
399 counter it (16). Since lytic cell death releases inflammatory mediators, its inhibition by ExoS likely
400 serves to limit host responses to infection while also preserving the replicative niche. If so, killing
401 cytosolic bacteria with antibiotics that preserve the vacuolar population could favor immune
402 responses/inflammation. How this would play out in an actual infection (e.g. increased bacterial
403 clearance versus damaging inflammation) will require further investigation given the complexities
404 of *in vivo* systems. An additional consideration relates to the design of novel therapies (e.g.
405 targeting bacterial biofilms) if they need to access an intracellular niche enclosed by two host
406 membrane layers.

407 Intravital confocal imaging of infected mouse corneas was used to explore the location of *P.*
408 *aeruginosa* within cells after *in vivo* infection. The methods used allowed spatial and temporal
409 resolution, and therefore accurate localization of bacteria with respect to cell membranes over time
410 in addition to their depth within the tissue. Bacteria were detected in the cytosol of infected
411 epithelial cells, some deep within the tissue and others closer to the corneal surface. As we have
412 shown *in vitro*, this included multiple bacteria disseminating through the cell cytoplasm at
413 speeds/pattern aligning with twitching motility, with some cells (also or instead) containing rapidly
414 swimming bacteria inside membrane blebs. A third intracellular bacterial population was detected

415 resembling *P. aeruginosa*-containing vacuoles occurring in cultured epithelial cells. While the
416 fluorescent signal from bacteria packed inside vacuoles merges to prevent resolution of individual
417 bacteria, the circular shape of the emanating fluorescence implies that these bacterial-containing
418 regions are surrounded by a vacuolar membrane.

419 Mutants lacking the T3SS ($\Delta exsA$) remain in vacuoles because they lack the ability to escape
420 the vacuole. These were also found to express biofilm-associated factors, essentially phenocopying
421 T3SS-negative sub-populations of wild-type persisting in vacuoles. While showing that T3SS
422 mutants can be used to study the phenotype, this result also suggests that lack of T3SS expression
423 and subsequently the vacuolar environment may drive biofilm production. Biofilm production in
424 response to the vacuolar environment aligns with our current understanding of biofilms, which can
425 help bacteria tolerate adverse environmental conditions such as nutrient limitation, host immune
426 responses, and exposure to antibiotics (3, 4, 27, 31, 51, 52), and is therefore triggered by such
427 conditions. There are many aspects of the vacuole environment with the potential to trigger the
428 production of biofilm, including vacuolar acidification, expression of intracellular antimicrobial
429 factors such as defensin antimicrobial peptides, reactive oxygen species, and lytic enzymes which
430 all form part of the antimicrobial activity of phagolysosomes (53). Alternatively, biofilm
431 production in vacuoles might relate to the T3SS-off state. *P. aeruginosa* can switch back and forth
432 between T3SS-on/motile/rapid growth state and a T3SS-off/non-motile/biofilm-producing/slow
433 growth/antibiotic-tolerant state, which is controlled by a complex regulatory system (Gac/Rsm
434 pathway) (54). This is often referred to as the acute/chronic switch in infection because the former
435 supports acute infection pathogenesis, and the latter promotes persistence and chronic infection.
436 While features of the cytosolic versus vacuolar niches arising when *P. aeruginosa* diversifies
437 inside cells are reminiscent of the acute and chronic states, the latter are generally believed to occur

438 in different infection types, or at least different time points during infection. Here, we have found
439 the intracellular phenotypes occur simultaneously (including in the same cell) and they both occur
440 relatively early (acute T3SS^{on} 4 h and *cdrA*^{on} 6 h). Related to this, others have reported other
441 situations when the lines between acute and chronic infection phenotypes are blurred (55, 56).
442 More work will be needed to understand the relationship if any between intracellular diversity of
443 *P. aeruginosa* and previously described phenotypic switches.

444 Our data showed that *P. aeruginosa* in vacuoles expressed biofilm factors known to help it
445 persist in the host and other adverse environments. They were also more antibiotic-tolerant than
446 *P. aeruginosa* found elsewhere in the cell which did not express biofilm factors. Nevertheless,
447 mutants lacking the biofilm protein CdrA and all three biofilm-associated exopolysaccharides
448 retained their ability to persist in vacuoles and tolerate antibiotics, showing that these factors were
449 not required. Accordingly, only a sub-fraction of the vacuolar population expressed *cdrA* when
450 wild-type was used, and the total percentage of cells containing antibiotic-tolerant bacteria
451 exceeded the fraction expressing *cdrA*. While inconsistent *cdrA* expression might relate to different
452 stages of maturation in the vacuole, this result provides further evidence that *cdrA* is not required.

453 Possible explanations for these results include functional redundancy with other biofilm-
454 associated factors, or that different biofilm-associated factors are responsible - possibly even novel
455 biofilm factors produced in this location. Alternatively, persistence/antibiotic tolerance might not
456 be due to biofilm factors. Other possibilities include a reduced growth rate, which can decrease
457 sensitivity to fluoroquinolones (52). Division rates for vacuolar bacteria were obviously slower
458 than the rapid replication occurring in the cytosol (Fig. 3A, D and Fig. 5A), not surprising given
459 space and nutrient limitations, and other adverse conditions expected in vacuoles. Other
460 phenotypic changes that could participate include expression of multidrug efflux pumps or factors

461 that modulate cell wall permeability (57–59), or that vacuolar bacterial sub-population(s) enter a
462 persister state in the face of ofloxacin exposure (60). Rather than being a property of the enclosed
463 bacteria, enhanced tolerance in vacuoles might instead relate to vacuolar properties. While the
464 antibiotic is cell permeable, there will still be some exclusion by the vacuolar membrane. In this
465 regard, the concentration needed to kill cytosolic bacteria (enclosed by the host cell plasma
466 membrane) was somewhat higher than needed to kill extracellular bacteria (~2-fold). This alone is
467 unlikely to explain the ~4- to 8-fold additional tolerance of vacuolar bacteria on the other side of
468 a second membrane. However, it is possible that *P. aeruginosa*, like other intracellular vacuolar
469 bacteria, modifies the vacuolar membrane (46, 47, 61, 62). If such modification to the vacuolar
470 membrane limits penetration of antibiotics remains unknown. Since there are many possibilities,
471 pinpointing the mechanisms by which *P. aeruginosa* persists in vacuoles will require further
472 investigation, which could lead to novel strategies for treating antibiotic recalcitrant infections.

473 While studying the exopolysaccharide (EPS) mutants, we found that they persisted in cells
474 even more efficiently than wild-type, the results showing that they occupied ~25 – 30 % of cells
475 versus ~15-20 % of cells for wild-type or *cdrA* mutants able to express EPS (Fig. 6C and D, grey
476 bars). Interestingly, initial internalization (at 4 h) of wild-type and Δ EPS mutants was similar
477 (Supplemental Fig. S2) suggesting that greater intracellular persistence of Δ EPS mutants at 12 h
478 (Fig. 6C, D) was not due to loss of antiphagocytic activity, the latter being a well-established role
479 for exopolysaccharides in other types of bacteria. However, determining how EPS contributes to
480 modification of bacterial persistence was beyond the scope our aims.

481 This study further demonstrates the advantage of time-lapse imaging for studying intracellular
482 bacterial populations, particularly for those with a complex lifestyle. For instance, the detection
483 and quantification of fluorescent bacteria using gene-expression reporters allowed the delineation

484 of viable intracellular sub-populations in real-time. Moreover, this methodology is especially of
485 value when studying bacterial persistence after antibiotic treatment as it can detect metabolically-
486 active bacteria that may not be quantifiable using traditional CFU counting, e.g. viable but non-
487 culturable cells. Another advantage of imaging, labeling cellular structures, use of high-resolution
488 methods, and including temporal information, is being able to distinguish intracellular bacteria
489 from antibiotic recalcitrant extracellular bacteria, which can occur if bacteria form extracellular
490 biofilms around the cells being studied (63, 64). A potential *caveat* of our study relates to the
491 arabinose-inducible GFP expression method we used to visualize all intracellular bacteria
492 irrespective of gene expression profile. Recent studies have shown that with some promoters,
493 including the one used here, expression can be impacted by Vfr (65, 66), in which case the number
494 of intracellular bacteria might be greater than those we detected using this method.

495 In conclusion, this study furthers our understanding of the intracellular lifestyle of *P.*
496 *aeruginosa* by demonstrating that it diversifies intracellularly to form viable sub-populations in
497 both vacuoles and the cytoplasm of epithelial cells. In these distinct locations they adopt different
498 phenotypes and functions. T3SS-expressing bacteria exit vacuoles, disseminate through the
499 cytoplasm using twitching motility, and use ExoS to replicate rapidly, avoid autophagy, and inhibit
500 cell death to keep the replicative niche alive. Some of these T3SS-expressing cytosolic bacteria
501 also use ExoS to assemble and occupy membrane bleb niches that can subsequently detach,
502 allowing vesicle-contained T3SS-expressing bacteria to travel to distant locations (9). Meanwhile,
503 vacuolar populations in the same or adjacent cells grow slowly, express biofilm-associated factors,
504 tolerate antibiotics, and in the absence of cytosolic cell-mates trigger death of the infected host
505 cell. Since the different phenotypes can occur in the same cell, cooperation is likely and might
506 ensure both short- and long-term interests are met. Other bacteria able to adopt an intracellular

507 lifestyle tend to establish one type of niche in an infected cell type, even if they traffic through
508 various compartments to arrive there. The unique ability of *P. aeruginosa* to diversify
509 intracellularly and assemble multiple niches associated with differential gene expression is likely
510 to contribute to the reasons why it is a highly effective opportunistic pathogen, and why infections
511 caused by it are so difficult to treat.

512

513 MATERIALS AND METHODS

514

515 **Cell culture.** Human corneal epithelial cells (hTCEpi) (67) were cultured in KGM-2 (Lonza, USA)
516 supplemented with 1.15 mM calcium chloride (high-calcium) to allow differentiation and
517 maintained at 37°C (humidified) in a 5 % CO₂ incubator. Human bronchial epithelial cells (NuLi-
518 1) were cultured as previously described (19) in BEGM (Lonza, USA) with 1.15 mM calcium
519 chloride and maintained as for hTCEpi. Epithelial cells were grown as monolayers on 24-well
520 tissue culture dishes (MatTek Corporation, Ashland, MA) for wide-field microscopy or plasmid
521 validation respectively, or on 8-well tissue culture dishes (ibidi, Gräfelfing, Germany) or glass-
522 coverslips for use in immunofluorescence.

523

524 **Bacterial strains, plasmids, and mutants.** *P. aeruginosa* strains and plasmids are shown in Table
525 1. Bacteria were grown at 37 °C on trypticase soy agar (TSA) (Hardy Diagnostics, Santa Maria,
526 CA) for 16 h before use. For imaging bacteria were transformed with either the T3SS-GFP reporter
527 (pJNE05), c-di-GMP Turbo-RFP reporter (pFy4535)(39), *cdrA*-GFP reporter (pMG078), or
528 pBAD-GFP (arabinose-inducible, pGFP_{arabinose}) and grown on media supplemented with
529 gentamicin (100 µg/mL). Bacterial inocula were prepared by resuspending bacterial colonies into

530 sterile PBS to an optical density (O.D) at 550 nm of 1.0 ($\sim 2 \times 10^8$ CFU/mL).

531 To construct plasmid pMG078 (*cdrA*-GFP), the pJNE05 empty vector was engineered to have
532 a promoter-less *gfp* and adding MluI and ScaI restriction sites upstream of the *gfp* to create a
533 multiple cloning site for introducing any promoter of interest. Briefly, pJNE05 was prepared as
534 two large PCR products with overlapping ends, with the MluI and ScaI sites added to the primers
535 and excluding the promoter already present in the native pJNE05 vector. Fragment 1 was amplified
536 using the primer pair with engineered restriction sites indicated in bold pJNE05_part1.1a and
537 pJNE05_part1.1b- and Fragment 2 was amplified using pJNE05_part2.1a and pJNE05_part2.1b
538 (Table 2). The two fragments with overlapping ends were assembled by Gibson assembly. The
539 *cdrA* promoter region for the promoter-*gfp* fusion was then amplified using previously published
540 primers (68) with slight modification for our vector backbone (cdrA.1a and cdrA.1b, Table 2). The
541 resulting fragment and promoter-less *gfp*-pJNE05 backbone were digested with MluI and ScaI
542 then fused by T4 DNA ligase to construct the pMG078 vector. The prepared *cdrA*-GFP fusion
543 reporter was confirmed by comparing relative fluorescence intensity in WT (PAO1F) and the
544 PAO1F Δ *fleQ* mutant (11) in the stationary phase of batch culture after \sim 12 h growth in TSB at
545 37°C (normalized to O.D. at 650 nm) (Supplemental Figure S1A). Sensitivity of the *cdrA*-GFP
546 reporter (pMG078) to high levels of c-di-GMP was determined by comparing relative fluorescence
547 intensity in wild-type (PAO1P; low c-di-GMP) and the mutant PAO1P Δ *wspF* (hi-c-di-GMP) over
548 24 h of growth in TSB at 37°C in a Biotek plate reader at 200 rpm recording every 30 min
549 (Supplemental Figure S1B).

550 To construct pBAD-GFP (pGFP_{arabinose}), the promoter region of the pJNE05 was replaced with
551 an arabinose-inducible promoter region. The *exoS* promoter of pJNE05 was excised by digesting
552 with HindIII and EcoRI and replaced with the arabinose-inducible promoter from plasmid pTJ1.

553 Validation of pGFP_{arabinose} *in-vitro* was performed using hTCEpi cultured on 24-well plates.
554 Epithelial cells were inoculated with PAO1F::pGFP_{arabinose} or PAO1FD_{exsA}::pGFP_{arabinose} (~2 x
555 10⁶CFU bacteria, MOI of 10) for 3 h. Extracellular bacteria killed by adding amikacin (200 µg/mL)
556 for 30 min. GFP expression was induced after 30 min by adding media containing 1% L-arabinose
557 and the GFP signal recorded hourly for 8 h on a Nikon Ti Eclipse inverted wide-field microscope
558 (Supplemental Fig. S1).

559 Plasmid pMG055 (constitutive blue fluorescent protein, EBFP2) was constructed as follows.
560 Briefly, to start pMG046 was generated by cloning the tac promoter and dtomato from p67T1 (69)
561 and cloned into the AscI/NotI site of pTJ1. *Ebfp2* from the plasmid pBAD-*ebfp2* (purchased from
562 Addgene) was then cloned into the BamHI/HindIII site of pMG046 downstream of the tac
563 promoter (replacing dTomato) to create pMG051. Then, the ptac-*ebfp2* construct was amplified
564 from pMG051, plus the T0T1 terminator fragment amplified from pTJ1, and cloned via Gibson
565 assembly into the SalI/BamHI site of promoter-less GFP pJNE05 based plasmid, to yield pMG055
566 - which has a constitutive EBFP2, and a promoter-less *gfp* gene.

567
568 **Bacterial internalization assays.** Epithelial cells were inoculated with 5 µl (containing ~2 x 10⁶
569 CFU bacteria) of a suspension of *P. aeruginosa* PAO1 wild-type or mutants transformed with
570 fluorescent reporter plasmids (MOI = 10) and incubated for 3 h at 37 °C (internalization period).
571 Epithelial cells were then incubated with cell culture medium (KGM-2 or BEGM + 1.15 mM
572 calcium) supplemented with amikacin (200 µg/mL) for 1 h to kill extracellular bacteria. To explore
573 ofloxacin susceptibility of intracellular bacteria, epithelial cells were exposed to both amikacin
574 (200 µg/mL) and ofloxacin at concentrations ranging from the MIC to 16X MIC. Controls were
575 treated with cell culture media including matched levels of acetic acid diluent. In some experiments,

576 pGFP_{arabinose} was activated 30 min after extracellular antibiotic was administered using 1 % L-
577 arabinose.

578

579 **Microscopy.** Live and time-lapse images were captured on a Nikon Ti-E inverted wide-field
580 fluorescence microscope equipped with Lumencor SpectraX illumination source and Okolab Uno-
581 combined controller stage top incubation chamber to maintain heat, humidity, and 5 % CO₂. Time-
582 lapse images were captured using a CFI Plan Apo Lambda 40X air objective, equipped with
583 differential interference contrast (DIC). Live phase-contrast images were captured using a Plan
584 Apo Lambda Ph3DM 60X oil-immersion objective. For time-lapse, fields were chosen visualizing
585 DIC only to identify areas free of debris; Turbo-RFP and GFP were not observed until time-lapse
586 was completed to avoid bias in field selection. For time-lapse imaging with quantification, eight
587 fields were imaged for each condition. For live phase-contrast without quantification, three fields
588 were imaged for each condition.

589

590 **Ofloxacin stock solutions and determination of MIC.** Target ofloxacin concentrations from
591 0.0625 - 8 µg/mL were obtained by dilution of a 10 mg/mL stock solution (prepared in 100 %
592 acetic acid) in cell culture media. Concentrations of 16 - 64 µg/mL were prepared by diluting a 6.4
593 mg/mL stock solution (prepared in 10 % acetic acid) by 1:400 to 1:100. Similarly, a concentration
594 of 25 µg/mL was prepared by diluting a 2.5mg/mL stock solution (prepared in 10 % acetic acid)
595 by 1:100 dilution. Dilutions were such that acetic acid levels in each assay were below 0.1 %. The
596 MIC of ofloxacin against *P. aeruginosa* wild-type and mutant strains was determined by
597 inoculating ~1.5 x 10⁸ CFU of bacteria in tryptic soy broth into a 96-well plate at 37 °C, then
598 incubating overnight (16 h) in the presence of ofloxacin at the above concentrations. The MIC was

599 determined as the lowest concentration that inhibited bacterial growth measured by absorbance at
600 550 nm.

601
602 **Immunofluorescence.** Epithelial cells were cultured and inoculated with bacteria as described
603 above. After 3 h, KGM-2 (+ 1.15 mM calcium) containing amikacin (200 μ g/mL) was added to
604 kill extracellular bacteria for 3 h at 37 °C or amikacin with ofloxacin (up to 16X MIC) added to
605 also challenge intracellular bacteria. At 6 h post-inoculation, cells were washed with PBS, and
606 fixed in fresh 4 % paraformaldehyde (PFA) (Sigma-Aldrich) for 10 min. After an additional PBS
607 wash, cells were permeabilized for 10 min using 4 % PFA containing 0.1 % Triton X-100. Cells
608 were quenched with aldehydes in 150 mM glycine (Sigma-Aldrich) for 10 min, washed in PBS,
609 and blocked for 1 h at room temperature in 0.7 % fish skin gelatin (Sigma-Aldrich). All *P.*
610 *aeruginosa* bacteria were labeled with anti-*Pseudomonas* antibody (Abcam, #ab74980, primary)
611 with Alexa-Fluor 555 (Sigma, secondary) for 1 h. For all preparations: cells were washed with
612 PBS, ProLong™ Diamond Antifade Mounting Medium (ThermoFisher Scientific) was applied
613 and samples were sealed with a coverslip and imaged. Epithelial cell nuclei were stained with
614 NucBlue® Live ReadyProbes® Reagent (ThermoFisher Scientific).

615
616 **Correlative Light and Electron Microscopy (CLEM).** The hTCEpi were grown to 70 %
617 confluence on 35 mm grided Mattek™ dishes with a glass bottom by adding $\sim 6 \times 10^5$ cells in
618 KGM-2 media containing 1.15 mM calcium chloride and incubating overnight in a cell culture
619 incubator. Prior to infection, Hoechst dye was added at a concentration of 3 μ l/mL to stain the
620 nuclei. Epithelial cells were infected with bacteria at an MOI of 10 and allowed to progress for 3
621 h. At this time, 1:1 dilution of prewarmed amikacin (400 μ g/mL) in KGM-2 + 1.15 mM calcium

622 was added for 30 min followed by ofloxacin to a final concentration of 1 µg/mL for 3 h (total
623 infection time = 6 h). At 6 h, 2 mL of media was removed leaving 1 mL behind to prevent cells
624 drying. Cells were washed three times with the sequential addition of 1 mL of cell culture media
625 always leaving behind 1 mL. Cells were fixed with 1 mL of fixative media in KGM-2 (8 % electron
626 microscopy grade paraformaldehyde [PFA]) for a minimum of 30 min. All fluorescent images
627 were obtained in PFA-containing media. Following fluorescence imaging, cells were fixed in 2.5%
628 glutaraldehyde and 2.5% paraformaldehyde in 0.1M sodium cacodylate buffer, pH 7.4 (EMS,
629 Hatfield, PA, USA). Samples were rinsed 3 times (5 min each) at room temperature) in 0.1M
630 sodium cacodylate buffer, pH 7.2, and immersed in 1% osmium tetroxide with 1.6% potassium
631 ferricyanide in 0.1M sodium cacodylate buffer for 30 min. Samples were rinsed 3 times (5 min
632 each) at room temperature in buffer and briefly washed once with distilled water (1 min) at room
633 temperature. Samples were then subjected to an ascending ethanol gradient followed by pure
634 ethanol. Samples were then progressively infiltrated (using ethanol as solvent) with Epon resin
635 (EMS, Hatfield, PA, USA) and polymerized at 60 °C for 24 - 48 h. Care was taken to ensure only
636 a thin amount of resin remained within the glass bottom dishes to enable the best possible chance
637 for separation of the glass coverslip. Following polymerization, the glass coverslips were removed
638 using ultra-thin Personna razor blades (EMS, Hatfield, PA, USA) and liquid nitrogen exposure, as
639 needed. Correlative Light and Electron Microscopy (CLEM), was performed to visualize specific
640 cells of interest. Regions of interest, identified by the gridded alpha-numerical labeling on the
641 plates were carefully removed, precisely trimmed to the cell of interest, and mounted on a blank
642 resin block with cyanoacrylate glue for sectioning. Serial thin sections (80 nm) were cut using a
643 Leica UC6 ultramicrotome (Leica, Wetzlar, Germany) from the surface of the block until
644 approximately 4-5 microns within to ensure complete capture of the cell volumes. Section-ribbons

645 were then collected sequentially onto formvar-coated slot- or 50-mesh grids. The grids were post-
646 stained with 2% uranyl acetate followed by Reynold's lead citrate, for 5 min each. Sections were
647 imaged using a FEI Tecnai 12 120kV TEM (FEI, Hillsboro, OR USA) and data recorded using
648 either a Gatan US1000 CCD with Digital Micrograph 3 or a Gatan Rio 16 CMOS with Gatan
649 Microscopy Suite software (Gatan Inc., Pleasanton, CA, USA).

650

651 **Murine infection model.** All procedures involving animals were carried out in accordance with
652 the standards established by the Association for the Research in Vision and Ophthalmology, under
653 a protocol AUP-2019-06-12322 approved by the Animal Care and Use Committee, University of
654 California Berkeley. This protocol adheres to PHS policy on the humane care and use of laboratory
655 animals, and the guide for the care and use of laboratory animals. For *in-vivo* imaging of corneal
656 infection by *P. aeruginosa*, 8-10 week old female C57BL/6 Lyz2cre+/mRosa-DTR mice (F1
657 cross) were used since they express red fluorescent membranes and green/yellow myeloid-derived
658 cells. The cornea scarification model was used to establish infection as previously described (70,
659 71). Briefly, mice were anesthetized for 4 h by ketamine-dexmedetomidine injection (ketamine
660 80-100mg/Kg and dexmedetomidine 0.25-0.5 mg/Kg) and the cornea of one eye scratched in
661 parallel three times with a sterile 26 G needle, then inoculated with 5 μ L of wild-type mPAO1-
662 EBF2 (pMG055; constitutive blue fluorescent protein) in suspension containing $\sim 10^9$ CFU of
663 bacteria at 1 h intervals for 4 h while under continued anesthesia ketamine-dexmedetomidine
664 injection. After 4 h, mice were woken up with anesthesia reversal agent Atipamezole via injection
665 (2.5 – 5 mg/Kg) and remained under supervision for 10 h. At 15 h, mice were re-anesthetized
666 ketamine-dexmedetomidine injection (ketamine 80-100mg/Kg and dexmedetomidine 0.25-0.5
667 mg/Kg) and infected corneas imaged in the live animals by confocal microscopy.

668

669 **Statistical analysis.** Prism software was used for numerical data analysis. Data were expressed as
670 a mean +/- standard deviation (SD). Two group comparisons were performed using Student's t-
671 Test, and multiple group analysis was performed using One-way ANOVA with Dunnett's multiple
672 comparisons test. *P* values less than 0.05 were considered significant.

673

674 **Funding Information**

675 This work was supported by the National Institutes of Health; R01 EY011221 (SMJF), F32
676 EY029152 (VN) and F32 EY025969 (ARK), by the Elizabeth Nash Memorial Fellowship awarded
677 by Cystic Fibrosis Research Inc. (NGK), and the American Heart Association (MG). The funding
678 agencies had no role in the study design, data collection and interpretation, or decision to submit
679 the work for publication.

680

681 **Acknowledgements**

682 Thanks to Dr. Alain Filloux (Imperial College London, UK), Dr. Fitnat Yildiz (University of
683 California Santa Cruz, CA) and Dr. Matthew Parsek (University of Washington, WA) for
684 providing *P. aeruginosa* wild-type strains, respective mutants and plasmid constructs. Thanks to
685 Dr. Danielle Robertson (University of Texas Southwestern, TX) for providing the telomerase-
686 immortalized human corneal epithelial cells. Thanks to Dr. Danielle Jorgens and Ms. Reena
687 Zalpuri at the University of California Berkeley Electron Microscope Laboratory for expert advice
688 and assistance with electron microscopy.

689

690 **Contributions**

691 NGK, VN, ARK, MG, MM, TY, DE and SF designed experiments; NGK, VN, ARK, EJ, MH,
692 MG and MM performed the experiments; NGK, VN, ARK, MG, MM, TY, DE and SF analyzed
693 and interpreted the data; NGK, VN, ARK, DE and SF wrote the manuscript; DE and SF supervised
694 the study.

695 **References**

696

697 1. Sader HS, Huband MD, Castanheira M, Flamm RK. 2017. *Pseudomonas aeruginosa*
698 antimicrobial susceptibility results from four years (2012 to 2015) of the International
699 Network for Optimal Resistance Monitoring Program in the United States. *Antimicrob
700 Agents Chemother* 61:e02252-16.

701 2. Mulcahy LR, Isabella VM, Lewis K. 2014. *Pseudomonas aeruginosa* biofilms in disease.
702 *Microb Ecol* 68:1-12.

703 3. Moradali MF, Ghods S, Rehm BHA. 2017. *Pseudomonas aeruginosa* lifestyle: A paradigm
704 for adaptation, survival, and persistence. *Front Cell Infect Microbiol* 7:39.

705 4. Winstanley C, O'Brien S, Brockhurst MA. 2016. *Pseudomonas aeruginosa* evolutionary
706 adaptation and diversification in cystic fibrosis chronic lung infections. *Trends Microbiol*
707 24:327-337.

708 5. Fleiszig SMJ, Kroken AR, Nieto V, Grosser MR, Wan SJ, Metruccio MME, Evans DJ.
709 2019. Contact lens-related corneal infection: Intrinsic resistance and its compromise. *Prog
710 Retin Eye Res* 76: 100804.

711 6. Fleiszig SM, Zaidi TS, Fletcher EL, Preston MJ, Pier GB. 1994. *Pseudomonas aeruginosa*
712 invades corneal epithelial cells during experimental infection. *Infect Immun* 62:3485-3493.

713 7. Fleiszig SM, Zaidi TS, Pier GB. 1995. *Pseudomonas aeruginosa* invasion of and
714 multiplication within corneal epithelial cells in vitro. *Infect Immun* 63:4072-4077.

715 8. Fleiszig SMJ, Zaidi TS, Preston MJ, Grout M, Evans DJ, Pier GB. 1996. Relationship
716 between cytotoxicity and corneal epithelial cell invasion by clinical isolates of
717 *Pseudomonas aeruginosa*. *Infect Immun* 64:2288-2294.

718 9. Angus AA, Lee AA, Augustin DK, Lee EJ, Evans DJ, Fleiszig SMJ. 2008. *Pseudomonas*
719 *aeruginosa* induces membrane blebs in epithelial cells, which are utilized as a niche for
720 intracellular replication and motility. *Infect Immun* 76:1992-2001.

721 10. Heimer SR, Evans DJ, Stern ME, Barbieri JT, Yahr T, Fleiszig SMJ. 2013. *Pseudomonas*
722 *aeruginosa* utilizes the type III secreted toxin ExoS to avoid acidified compartments within
723 epithelial cells. *PLoS One* 8:e73111.

724 11. Kroken AR, Chen CK, Evans DJ, Yahr TL, Fleiszig SMJJ. 2018. The Impact of ExoS on
725 *Pseudomonas aeruginosa* Internalization by epithelial cells is independent of *fleQ* and
726 correlates with bistability of type three secretion system gene expression. *MBio* 9:e00668-
727 18.

728 12. Sana TG, Baumann C, Merdes A, Soscia C, Rattei T, Hachani A, Jones C, Bennett KL,
729 Filloux A, Superti-Furga G, Voulhoux R, Bleves S. 2015. Internalization of *Pseudomonas*
730 *aeruginosa* strain PAO1 into epithelial cells is promoted by interaction of a T6SS effector
731 with the microtubule network. *MBio* 6: 00712-15.

732 13. Fleiszig SM, Wiener-Kronish JP, Miyazaki H, Vallas V, Mostov KE, Kanada D, Sawa T,
733 Yen TS, Frank DW. 1997. *Pseudomonas aeruginosa*-mediated cytotoxicity and invasion
734 correlate with distinct genotypes at the loci encoding exoenzyme S. *Infect Immun* 65:579-
735 586.

736 14. Zaidi TS, Fleiszig SM, Preston MJ, Goldberg JB, Pier GB. 1996. Lipopolysaccharide outer
737 core is a ligand for corneal cell binding and ingestion of *Pseudomonas aeruginosa*. *Invest*
738 *Ophthalmol Vis Sci* 37:976-986.

739 15. Hritonenko V, Evans DJJ, Fleiszig SMJM. 2012. Translocon-independent intracellular
740 replication by *Pseudomonas aeruginosa* requires the ADP-ribosylation domain of ExoS.

741 *Microbes Infect* 14:1366-1373.

742 16. Kroken AR, Gajenthra Kumar N, Yahr TL, Smith BE, Nieto V, Horneman H, Evans DJ,
743 Fleiszig SMJ. 2022. Exotoxin S secreted by internalized *Pseudomonas aeruginosa* delays
744 lytic host cell death. *PLoS Pathog* 18:e1010306.

745 17. Angus AA, Evans DJ, Barbieri JT, Fleiszig SMJ. 2010. The ADP-ribosylation domain of
746 *Pseudomonas aeruginosa* ExoS is required for membrane bleb niche formation and
747 bacterial survival within epithelial cells. *Infect Immun* 78:4500-4510.

748 18. Cowell BA, Chen DY, Frank DW, Vallis AJ, Fleiszig SMJ. 2000. ExoT of cytotoxic
749 *Pseudomonas aeruginosa* prevents uptake by corneal epithelial cells. *Infect Immun* 68:403-
750 406.

751 19. Jolly AL, Takawira D, Oke OO, Whiteside SA, Chang SW, Wen ER, Quach K, Evans DJ,
752 Fleiszig SMJ. 2015. *Pseudomonas aeruginosa*-induced bleb-niche formation in epithelial
753 cells is independent of actinomyosin contraction and enhanced by loss of cystic fibrosis
754 transmembrane-conductance regulator osmoregulatory function. *MBio* 6:e02533.

755 20. Evans DJ, Frank DW, Finck-Barbançon V, Wu C, Fleiszig SMJ. 1998. *Pseudomonas*
756 *aeruginosa* Invasion and Cytotoxicity Are Independent Events, Both of Which Involve
757 Protein Tyrosine Kinase Activity. *Infect Immun* 66:1453-1459.

758 21. Diaz MR, King JM, Yahr TL. 2011. Intrinsic and extrinsic regulation of type III secretion
759 gene expression in *Pseudomonas aeruginosa*. *Front Microbiol* 2:89.

760 22. Garai P, Berry L, Moussouni M, Bleves S, Blanc-Potard A-B. 2019. Killing from the inside:
761 Intracellular role of T3SS in the fate of *Pseudomonas aeruginosa* within macrophages
762 revealed by *mgtC* and *oprF* mutants. *PLOS Pathog* 15:e1007812.

763 23. Rao L, De La Rosa I, Xu Y, Sha Y, Bhattacharya A, Holtzman MJ, Gilbert BE, Eissa NT.

764 2021. *Pseudomonas aeruginosa* survives in epithelia by ExoS-mediated inhibition of
765 autophagy and mTOR. *EMBO Rep* 22:1-15.

766 24. Goldberg MB. 2001. Actin-based motility of intracellular microbial pathogens. *Microbiol*
767 *Mol Biol Rev* 65:595-626.

768 25. Nieto V, Kroken AR, Grosser MR, Smith BE, Metruccio MME, Hagan P, Hallsten ME,
769 Evans DJ, Fleiszig SMJ. 2019. Type IV Pili can mediate bacterial motility within epithelial
770 cells. *MBio* 10:e02880-18.

771 26. López D, Vlamakis H, Kolter R. 2010. Biofilms. *Cold Spring Harb Perspect Biol*
772 2:a000398.

773 27. Donlan RM, Costerton JW. 2002. Biofilms: survival mechanisms of clinically relevant
774 microorganisms. *Clin Microbiol Rev* 15:167-193.

775 28. Lyczak JB, Cannon CL, Pier GB. 2002. Lung infections associated with cystic fibrosis. *Clin*
776 *Microbiol Rev* 15:194-222.

777 29. Drenkard E, Ausubel FM. 2002. *Pseudomonas* biofilm formation and antibiotic resistance
778 are linked to phenotypic variation. *Nature* 416:740-743.

779 30. Wagner VE, Iglewski BH. 2008. *P. aeruginosa* biofilms in CF infection. *Clin Rev Allergy*
780 *Immunol* 35:124-134.

781 31. Whiteley M, Bangera MG, Bumgarner RE, Parsek MR, Teitzel GM, Lory S, Greenberg EP.
782 2001. Gene expression in *Pseudomonas aeruginosa* biofilms. *Nature* 413:860-864.

783 32. Colvin KM, Irie Y, Tart CS, Urbano R, Whitney JC, Ryder C, Howell PL, Wozniak DJ,
784 Parsek MR. 2012. The Pel and Psl polysaccharides provide *Pseudomonas aeruginosa*
785 structural redundancy within the biofilm matrix. *Environ Microbiol* 14:1913-1928.

786 33. Ryder C, Byrd M, Wozniak DJ. 2007. Role of polysaccharides in *Pseudomonas aeruginosa*

787 biofilm development. *Curr Opin Microbiol* 10:644-648.

788 34. Borlee BR, Goldman AD, Murakami K, Samudrala R, Wozniak DJ, Parsek MR. 2010.

789 *Pseudomonas aeruginosa* uses a cyclic-di-GMP-regulated adhesin to reinforce the biofilm

790 extracellular matrix. *Mol Microbiol* 75:827-842.

791 35. Reichhardt C, Wong C, da Silva DP, Wozniak DJ, Parsek MR. 2018. CDRA interactions

792 within the *Pseudomonas aeruginosa* biofilm matrix safeguard it from proteolysis and

793 promote cellular packing. *MBio* 9. e01376-18.

794 36. Jennings LK, Storek KM, Ledvina HE, Coulon C, Marmont LS, Sadovskaya I, Secor PR,

795 Tseng BS, Scian M, Filloux A, Wozniak DJ, Howell PL, Parsek MR. 2015. Pel is a cationic

796 exopolysaccharide that cross-links extracellular DNA in the *Pseudomonas aeruginosa*

797 biofilm matrix. *Proc Natl Acad Sci U S A* 112:11353-11358.

798 37. Okshevsky M, Meyer RL. 2015. The role of extracellular DNA in the establishment,

799 maintenance and perpetuation of bacterial biofilms. *Crit Rev Microbiol* 41:341-352.

800 38. Cherny KE, Sauer K. 2020. Untethering and degradation of the polysaccharide matrix are

801 essential steps in the dispersion response of *Pseudomonas aeruginosa* biofilms. *J Bacteriol*

802 202:e00575-19.

803 39. Zamorano-Sánchez D, Xian W, Lee CK, Salinas M, Thongsomboon W, Cegelski L, Wong

804 GCL, Yildiz FH. 2019. Functional specialization in *Vibrio cholerae* diguanylate. *MBio*

805 10:1-16.

806 40. Zhou H, Zheng C, Su J, Chen B, Fu Y, Xie Y, Tang Q, Chou SH, He J. 2016.

807 Characterization of a natural triple-tandem c-di-GMP riboswitch and application of the

808 riboswitch-based dual-fluorescence reporter. *Sci Rep* 6:1-13.

809 41. Reichhardt C, Jacobs HM, Matwichuk M, Wong C, Wozniak DJ, Parsek MR. 2020. The

810 versatile *Pseudomonas aeruginosa* biofilm matrix protein CdrA promotes aggregation
811 through different extracellular exopolysaccharide interactions. *J Bacteriol* 202:1-9.

812 42. Hsiao JY, Chen CY, Yang MJ, Ho HC. 2013. Live and dead GFP-tagged bacteria showed
813 indistinguishable fluorescence in *Caenorhabditis elegans* gut. *J Microbiol* 51:367-372.

814 43. Fredlund J, Santos JC, Stévenin V, Weiner A, Latour-Lambert P, Rechav K, Mallet A,
815 Krijnse-Locker J, Elbaum M, Enninga J. 2018. The entry of *Salmonella* in a distinct tight
816 compartment revealed at high temporal and ultrastructural resolution. *Cell Microbiol* 20:1-
817 13.

818 44. Bakkum T, Heemskerk MT, Bos E, Groenewold M, Oikonomou-Koppasis N, Walburg K
819 V., Van Veen S, Van Der Lienden MJC, Van Leeuwen T, Haks MC, Ottenhoff THM, Koster
820 AJ, Van Kasteren SI. 2020. Bioorthogonal correlative light-electron microscopy of
821 *Mycobacterium tuberculosis* in macrophages reveals the effect of antituberculosis drugs on
822 subcellular bacterial distribution. *ACS Cent Sci* 6:1997-2007.

823 45. Tam C, LeDue J, Mun JJ, Herzmark P, Robey EA, Evans DJ, Fleiszig SMJ. 2011. 3D
824 quantitative imaging of unprocessed live tissue reveals epithelial defense against bacterial
825 adhesion and subsequent traversal requires MyD88. *PLoS One* 6:e24008.

826 46. Kellermann M, Scharte F, Hensel M. 2021. Manipulation of host cell organelles by
827 intracellular pathogens. *Int J Mol Sci* 22:6484.

828 47. Case EDR, Smith JA, Ficht TA, Samuel JE, De Figueiredo P. 2016. Space: A final frontier
829 for vacuolar pathogens. *Traffic* 17:461-474.

830 48. Creasey EA, Isberg RR. 2014. Maintenance of vacuole integrity by bacterial pathogens.
831 *Curr Opin Microbiol* 17:46-52.

832 49. Chaudhary A, Miller SI. 2019. Xenophagy: Pathogen-containing vacuoles are hard to

833 digest. *Curr Biol* 29:R1086-R1088.

834 50. Rietsch A, Mekalanos JJ. 2006. Metabolic regulation of type III secretion gene expression
835 in *Pseudomonas aeruginosa*. *Mol Microbiol* 59:807-820.

836 51. Meluleni GJ, Grout M, Evans DJ, Pier GB. 1995. Mucoid *Pseudomonas aeruginosa*
837 growing in a biofilm in vitro are killed by opsonic antibodies to the mucoid
838 exopolysaccharide capsule but not by antibodies produced during chronic lung infection in
839 cystic fibrosis patients. *J Immunol* 155:2029-2038.

840 52. Evans DJ, Allison DG, Brown MRW, Gilbert P. 1991. Susceptibility of *Pseudomonas*
841 *aeruginosa* and *Escherichia coli* biofilms towards ciprofloxacin: Effect of specific growth
842 rate. *J Antimicrob Chemother* 27:177-184.

843 53. Nguyen JA, Yates RM. 2021. Better together: Current insights into phagosome-lysosome
844 fusion. *Front Immunol* 12:636078.

845 54. Zolfaghari I, Angus AA, Kang PJ, To A, Evans DJ, Fleiszig SMJ. 2005. Mutation of *retS*,
846 encoding a putative hybrid two-component regulatory protein in *Pseudomonas aeruginosa*,
847 attenuates multiple virulence mechanisms. *Microbes Infect* 7:1305-1316.

848 55. Mikkelsen H, Bond NJ, Skindersoe ME, Givskov M, Lilley KS, Welch M. 2009. Biofilms
849 and type III secretion are not mutually exclusive in *Pseudomonas aeruginosa*. *Microbiology*
850 155:687-698.

851 56. Wu YT, Tam C, Zhu LS, Evans DJ, Fleiszig SMJJ. 2017. Human Tear Fluid Reduces
852 culturability of contact lens-associated *Pseudomonas aeruginosa* biofilms but induces
853 expression of the virulence-associated type III secretion system. *Ocul Surf* 15:88-96.

854 57. Nikaido H. 2009. Multidrug resistance in bacteria. *Ann Rev Biochem* 78:119-146.

855 58. Mah T-FF, Pitts B, Pellock B, Walker GC, Stewart PS, O'Toole GA. 2003. A genetic basis

856 for *Pseudomonas aeruginosa* biofilm antibiotic resistance. *Nature* 426:306-310.

857 59. Masuda N, Ohya S. 1992. Cross-Resistance to meropenem, cephems, and quinolones in
858 *Pseudomonas aeruginosa*. *Antimicrob Agents Chemother* 36:1847-1851.

859 60. Barrett TC, Mok WWK, Murawski AM, Brynildsen MP. 2019. Enhanced antibiotic
860 resistance development from fluoroquinolone persisters after a single exposure to antibiotic.
861 *Nat Commun* 10:1177.

862 61. Stévenin V, Chang YY, Le Toquin Y, Duchateau M, Gianetto QG, Luk CH, Salles A, Sohst
863 V, Matondo M, Reiling N, Enninga J. 2019. Dynamic growth and shrinkage of the
864 *Salmonella*-ontaining vacuole determines the intracellular pathogen niche. *Cell Rep*
865 29:3958-3973.e7.

866 62. Padmanabhan B, Fielden LF, Hachani A, Newton P, Thomas DR, Cho HJ, Ai Khoo C,
867 Stojanovski D, Roy CR, Scott NE, Newton HJ. 2020. Biogenesis of the spacious *Coxiella*-
868 containing vacuole depends on host transcription factors TFEB and TFE3. *Infect Immun*
869 88:1-15.

870 63. Lepanto P, Bryant DM, Rossello J, Datta A, Mostov KE, Kierbel A. 2011. *Pseudomonas*
871 *aeruginosa* interacts with epithelial cells rapidly forming aggregates that are internalized by
872 a lyn-dependent mechanism. *Cell Microbiol* 13:1212-1222.

873 64. Wang S, Parsek MR, Wozniak DJ, Ma LZ. 2013. A spider web strategy of type IV pili-
874 mediated migration to build a fibre-like psl polysaccharide matrix in *Pseudomonas*
875 *aeruginosa* biofilms. *Environ Microbiol* 15:2238-2253.

876 65. Williams McMackin EA, Corley JM, Karash S, Marden J, Wolfgang MC, Yahr TL. 2021.
877 Cautionary notes on the use of arabinose- and rhamnose-inducible expression vectors in
878 *Pseudomonas aeruginosa*. *J Bacteriol* 203:e00224-21.

879 66. Almblad H, Harrison JJ, Rybtke M, Groizeleau J, Givskov M, Parsek MR, Tolker-Nielsen
880 T. 2015. The cyclic AMP-Vfr signaling pathway in *Pseudomonas aeruginosa* is inhibited
881 by cyclic Di-GMP. *J Bacteriol* 197:2190-2200.

882 67. Robertson DM, Li L, Fisher S, Pearce VP, Shay JW, Wright WE, Cavanagh HD, Jester J
883 V. 2005. Characterization of growth and differentiation in a telomerase-immortalized
884 human corneal epithelial cell line. *Investig Ophthalmol Vis Sci* 46:470-478.

885 68. Rybtke MT, Borlee BR, Murakami K, Irie Y, Hentzer M, Nielsen TE, Givskov M, Parsek
886 MR, Tolker-Nielsen T. 2012. Fluorescence-based reporter for gauging cyclic Di-GMP
887 levels in *Pseudomonas aeruginosa*. *Appl Environ Microbiol* 78:5060-5069.

888 69. Singer JT, Phennicie RT, Sullivan MJ, Porter LA, Shaffer VJ, Kim CH. 2010. Broad-Host-
889 Range Plasmids for Red Fluorescent Protein labeling of Gram-negative bacteria for use in
890 the Zebrafish model system. *Appl Environ Microbiol* 76:3467-3474.

891 70. Tam C, Lewis SEE, Li WYY, Lee E, Evans DJJ, Fleiszig SMJM. 2007. Mutation of the
892 phospholipase catalytic domain of the *Pseudomonas aeruginosa* cytotoxin ExoU abolishes
893 colonization promoting activity and reduces corneal disease severity. *Exp Eye Res* 85:799-
894 805.

895 71. Lee EJJ, Cowell BAA, Evans DJJ, Fleiszig SMJM. 2003. Contribution of ExsA-regulated
896 factors to corneal infection by cytotoxic and invasive *Pseudomonas aeruginosa* in a murine
897 scarification model. *Invest Ophthalmol Vis Sci* 44:3892-3898.

898 72. Jacobs MA, Alwood A, Thaipisuttikul I, Spencer D, Haugen E, Ernst S, Will O, Kaul R,
899 Raymond C, Levy R, Chun-Rong L, Guenthner D, Bovee D, Olson M V., Manoil C. 2003.
900 Comprehensive transposon mutant library of *Pseudomonas aeruginosa*. *Proc Natl Acad Sci
U S A* 100:14339-14344.

902 73. Urbanowski ML, Brutinel ED, Yahr TL. 2007. Translocation of ExsE into Chinese hamster
903 ovary cells is required for transcriptional induction of the *Pseudomonas aeruginosa* type III
904 secretion system. *Infect Immun* 75:4432-4439.

905

906

907 **Table Legends**

908

909 **Table 1.** *P. aeruginosa* strains, mutants and plasmids used in this study

910 **Table 2.** Primers used in this study

911

912 **Figure Legends**

913

914 **Figure 1. Intracellular wild-type *P. aeruginosa* form distinct phenotypes within human**

915 **epithelial cells. A)** Intracellular expression of genes encoding the T3SS (green), chronic switch

916 regulator c-di-GMP (red), or biofilm matrix protein CdrA (*cdrA*-GFP, pseudo-colored red) in

917 human corneal or bronchial epithelial cells at 6 h post-infection with *P. aeruginosa* PAO1F.

918 Extracellular bacteria were killed at 3 h post-infection with amikacin (200 µg/mL). T3SS-

919 expressing bacteria occupied the cytosol as expected. In contrast, bacteria reporting c-di-GMP or

920 *cdrA*-expression formed distinct localized vacuole-like niches within the same or different cells.

921 **B) and C)** 60 X oil-immersion phase-contrast microscopy shows *cdrA*-GFP reporting bacteria

922 (pseudo-colored red puncta) of wild-type PAO1F localized to vacuoles in corneal epithelial cells

923 (B) or bronchial epithelial cells (C). **D)** Percentage of corneal epithelial cells containing any

924 intracellular *P. aeruginosa* (PAO1F, black bar) and distinct *cdrA*-expressing phenotypes. After

925 labeling all bacteria with anti-*Pseudomonas* antibody, *cdrA*-GFP reporter expression allowed sub-
926 division of invaded cells into those only containing *cdrA*^{on} bacteria (red bar), only *cdrA*^{off} (green
927 bar), and those with both *cdrA*^{on} and *cdrA*^{off} (yellow bar). E) Percentage of corneal epithelial cells
928 containing intracellular PAO1FΔ*exsA* (black bar), a T3SS mutant that only localizes to vacuoles
929 (9). Cells containing *exsA* mutants showed a similar vacuolar distribution to wild-type with some
930 only containing *cdrA*^{on} (red bar) and others containing *cdrA*^{off} vacuolar bacteria (grey bar). In (D)
931 and (E), there was no significant difference between sub-groups in distribution of vacuolar
932 phenotypes (One-way ANOVA with Dunnett's multiple comparisons test). Data are shown as the
933 mean +/- SD of three biological replicates. Images below quantitative data in (D) and (E) show
934 examples of corneal epithelial cells for each of the categories quantified (bacteria pseudo-colored
935 as indicated: *cdrA*-GFP - magenta, anti-*Pseudomonas* antibody - cyan).

936

937 **Figure 2. CdrA is not required for host cell invasion and vacuolar localization.** A) Invasion
938 of corneal epithelial cells quantified by quantifying colony forming units (CFU) at 4 h post-
939 infection. Corneal cells were infected for 3 h with PAO1P and PAO1PΔ*cdrA*. Extracellular
940 bacteria were killed 3 h post-infection with amikacin (200 µg/mL) and cells lysed to recover
941 intracellular bacteria. B) Percentage of human corneal epithelial cells containing at least one *cdrA*^{on}
942 bacterial cell at 6 h post-infection. C) 60 X oil-immersion phase-contrast microscopy shows *cdrA*-
943 expressing bacteria (red puncta) of wild-type PAO1P and its mutant PAO1PΔ*cdrA* localized to
944 vacuoles in corneal or bronchial cells. White arrows point to bacteria in vacuoles. The same image
945 is shown with and without fluorescence. ns = Not Significant (Student's t-Test).

946

947 **Figure 3. Vacuolar *cdrA*^{on} populations show resistance to the cell permeable antibiotic**

948 **ofloxacin compared to cytosolic T3SS^{on} bacteria.** A) Images of human corneal epithelial cells
949 containing cytosolic T3SS-GFP-expressing PAO1F (T3SS^{on}) in the presence of ofloxacin (0.25 -
950 4 μ g/mL = 1 - 16X MIC) at 6 h and 12 h post-infection versus control. Extracellular bacteria were
951 killed after 3 h with the non-cell permeable amikacin (200 μ g/mL) (control) or amikacin
952 (200 μ g/mL) and ofloxacin were added at 3 h to also target intracellular bacteria. B-C) Percentage
953 of corneal epithelial cells containing at least one T3SS^{on} bacterial cell at 6 h (B) and 12 h (C) post-
954 infection under the above conditions. Increasing concentrations of ofloxacin eliminated most
955 cytosolic bacteria (* p < 0.05, ** p < 0.01, ns = Not Significant, One-way ANOVA with Dunnett's
956 multiple comparisons test). D) Images of *cdrA*-GFP-expressing PAO1F vacuolar bacteria (*cdrA*^{on})
957 in the presence of ofloxacin as above. Discrete foci of bacteria (green) persisted at 16X the MIC
958 of ofloxacin and at 12 h post-infection. E-F) Percentage of human corneal epithelial cells
959 containing at least one *cdrA*^{on} bacterial cell at 6 h (E) and 12 h (F) post-infection under the above
960 conditions. Increasing concentrations of ofloxacin failed to eliminate the *cdrA*^{on} vacuolar
961 population. No significant difference between groups (One-way ANOVA with Dunnett's multiple
962 comparisons test). Data shown as mean +/- SD of three biological replicates.

963

964 **Figure 4. Correlative light and electron microscopy of *cdrA*^{on} bacteria in vacuoles.**
965 Fluorescence and electron micrographs of human corneal epithelial cells at 6 h after inoculation
966 with PAO1F expressing *cdrA*-GFP. Extracellular bacteria were killed 3 h post-infection with
967 amikacin (200 μ g/mL) and amikacin (200 μ g/mL) and ofloxacin (1 μ g/mL) then added for a further
968 3 h. Cells were fixed at 6 h and fluorescence microscopy performed before preparing cells for
969 electron microscopy (EM). Red boxes show corneal epithelial cells with corresponding EM
970 micrographs. Black dotted boxes indicate regions from which respective insets were taken to show

971 bacteria within vacuoles with evidence of vacuolar membranes.

972

973 **Figure 5. The total population of ofloxacin-tolerant wild-type *P. aeruginosa* localizes to**
974 **vacuoles.** A) Images of human corneal epithelial cells containing PAO1F expressing pGFP_{arabinose}
975 to show all intracellular bacteria in the presence of ofloxacin (0.25 - 4 μ g/mL = 1 - 16X MIC) at 6
976 and 12 h post-infection versus control. After 3 h extracellular bacteria were killed with amikacin
977 (200 μ g/mL) (control) or amikacin (200 μ g/mL) and ofloxacin were added to also target
978 intracellular bacteria. Cytosolic PAO1F were cleared by ofloxacin at 1 μ g/mL at 6 h and by 0.5
979 μ g/mL at 12 h. Vacuolar bacteria persisted in the epithelial cells at 12 h post-infection at all
980 ofloxacin concentrations. B-C) Percentage of corneal epithelial cells containing at least one PAO1
981 with pGFP_{arabinose} bacterial cell at 6 h (B) and 12 h (C) post-infection under the above conditions.
982 Despite ofloxacin clearance of cytosolic bacteria, the percentage of cells containing intracellular
983 bacteria did not significantly differ between control and ofloxacin treated groups (One-way
984 ANOVA with Dunnett's multiple comparisons test). Data are shown as the mean +/- SD of three
985 biological replicates.

986

987 **Figure 6. Ofloxacin resistance of vacuolar *P. aeruginosa* does not require *cdrA* or**
988 **exopolysaccharide.** Percentage of human corneal epithelial cells containing intracellular *P.*
989 *aeruginosa* at 12 h post-infection with (A) PAO1P, (B) PAO1P Δ *cdrA*, (C) PAO1P Δ EPS
990 (Δ *pel* Δ *psl* Δ *algD*) or D) PAO1P Δ EPS Δ *cdrA*. Total intracellular bacteria were detected using
991 pGFP_{arabinose} (grey bars), and vacuolar *cdrA*^{on} using *cdrA*-GFP (red bars). Extracellular bacteria
992 were killed after 3 h with amikacin (200 μ g/mL) and amikacin (200 μ g/mL) and ofloxacin added
993 at 3 h (4 - 64 μ g/mL = 1 - 16X MIC). Intracellular bacteria persisted up to 16X MIC for wild-type

994 and mutants with a subset of each expressing *cdrA*. * p < 0.05, ** p < 0.01, *** p < 0.001, **** p
995 < 0.0001 (One Way ANOVA with Dunnett's multiple comparisons test versus untreated control).
996 Data are shown as mean +/- SD of three biological replicates.

997

998 **Figure 7. Vacuolar T3SS ($\Delta exsA$) mutants are also tolerant to ofloxacin.** A) Images of corneal
999 epithelial cells containing PAO1F $\Delta exsA$ (pGFP_{arabinose}) show that all intracellular bacteria are
1000 localized to vacuoles with or without ofloxacin (0.25 - 4 μ g/mL = 1 - 16X MIC) at 6 and 12 h post-
1001 infection. Extracellular bacteria were killed after 3 h with amikacin (200 μ g/mL) and then
1002 amikacin (200 μ g/mL) and ofloxacin added for a further 3 h. B) Percentage of corneal epithelial
1003 cells containing at least one bacterial cell at 6 h and 12 h post-infection under the above conditions.
1004 Increasing concentrations of ofloxacin failed to eliminate the *exsA* mutant vacuolar population at
1005 either time point. There was no significant difference between groups (One-way ANOVA
1006 with Dunnett's multiple comparisons test). C-D) Correlative light electron microscopy to visualize
1007 *exsA* mutants in vacuoles in the corneal epithelial cells at 6 h post infection in control (C) and
1008 ofloxacin (1 μ g/mL) treated (D) cells under the same conditions. Both insets show bacteria
1009 restricted to perinuclear vacuoles with evidence of a vacuolar membrane.

1010

1011 **Figure 8. Vacuolar *P. aeruginosa* contribute to host cell death.** Quantification of corneal
1012 epithelial cell death quantified using the ratio of PI/DAPI, also shown as the area under the curve
1013 (AUC) after internalization of *P. aeruginosa* PAO1F $\Delta exsA$ (A) from 4 to 20 h post-infection.
1014 Extracellular bacteria were killed after 3 h with non-cell permeable amikacin (200 μ g/mL) and
1015 ofloxacin added at 3 h (0.25 - 25 μ g/mL = 1 - 100 X MIC) with continued amikacin. Intracellular
1016 survival of bacteria shown as percentage of corneal epithelial cells containing a GFP-expressing

1017 bacterium (pGFP_{arabinose}) treated with 0 (no ofloxacin), 1 μ g/mL (4X MIC), 25 μ g/mL (100X MIC)
1018 at 12 h post-infection (B). The data show that ofloxacin-sensitive and ofloxacin-tolerant vacuolar
1019 bacteria both contribute to host cell death. * p < 0.05, ns = Not Significant (One-way ANOVA
1020 with Dunnett's multiple comparisons test versus untreated control).

1021

1022 **Figure 9. Intracellular cytosolic and vacuolar phenotypes of *P. aeruginosa* both occur *in vivo***
1023 **during corneal infection.** Corneal image of a Lyz2cre⁺/mRosa-DTR mouse (red fluorescent
1024 membranes with green/yellow myeloid-derived cells) at 15 h post-infection with *P. aeruginosa*
1025 mPAO1 expressing pMG055 (EBFP2 [blue], pseudo-colored cyan) using the murine scarification
1026 model. Confocal images were taken in the middle of the infected cornea scratch on an anesthetized
1027 live mouse. Insets show cytosolic bacteria spreading in the cell and/or within membrane blebs, and
1028 vacuolar bacteria (blue puncta) within neighboring cells. Side panels show lateral projections of
1029 imaging into the epithelium.

1030

1031 **Supplemental Information**

1032

1033 **Supplemental Figure S1.** Validation of *cdrA*-GFP and *pGFP_{arabinose}* reporters. A) Maximum
1034 fluorescence intensity (Relative Fluorescence Units, RFU) of the *cdrA*-GFP reporter (pMG078) in
1035 PAO1F and PAO1F Δ fleQ normalized to growth (O.D. at 650 nm) in the stationary phase (after
1036 ~12 h growth in TSB). B) Responsiveness of pMG078 to c-di-GMP levels. GFP fluorescence
1037 intensity normalized to O.D. at 550 nm of PAO1P (low-c-di-GMP) (black circles) and
1038 PAO1P Δ wspF (hi-c-di-GMP) (green squares) over 24 h growth at 30 min intervals. C) Inducible-
1039 GFP expression by intracellular PAO1F or its Δ exsA mutant (vacuolar) in human corneal epithelial

1040 cells using 1 % arabinose. Extracellular bacteria were killed with amikacin 200 μ g/mL at 3 h post-
1041 infection and cells imaged at 1 h intervals from 4 - 7 h. Color gradient shows the intensity of GFP
1042 expression. D) Upper panels show growth (O.D. at 550 nm) of wild-type *P. aeruginosa* parent
1043 strains transformed with *pGFP_{arabinose}* over 16 h. PAO1P (blue) or PAO1F (red) alone (closed
1044 symbols) or with 1 % arabinose (open symbols). Lower panels show concomitant recording of
1045 GFP intensity.

1046

1047 **Supplemental Fig. S2.** Bacterial internalization control experiments. Invasion of wild-type
1048 PAO1F and PAO1P into human corneal epithelial cells at 4 h post-infection (left panel) compared
1049 to PAO1P (WT) and its mutants in *cdrA*, EPS, or both (right panel) as determined by amikacin
1050 exclusion assay. Bars represent mean +/- SD of three biological replicates. ns = Not Significant
1051 (Student's t-Test, left panel; One-way ANOVA with Dunnett's multiple comparisons test, right
1052 panel).

1053

1054 **Supplemental Video Legends**

1055

1056 **Supplemental Video S1.** Time-lapse imaging of human corneal epithelial cells infected with
1057 PAO1F expressing pJNE05 (T3SS-GFP) showing T3SS^{on} bacteria from 4 - 24 h post-infection.
1058 Cells were infected with bacteria at an MOI of 10 and incubated for 3 h. At 3 h, antibiotic-
1059 containing media was added to kill extracellular bacteria only (amikacin, 200 μ g/mL) or
1060 extracellular and intracellular bacteria (amikacin, 200 μ g/mL and ofloxacin, 0.25 - 4 μ g/mL [1-
1061 16X MIC]). Cells were imaged at 1 h intervals for 20 h. Blue = Hoechst staining of nuclei (added
1062 during the incubation period), Red = Propidium Iodide staining (added at 3 h to stain dead host

1063 cells), Green = bacteria expressing GFP.

1064

1065 **Supplemental Video S2.** Time-lapse imaging of human corneal epithelial cells infected with
1066 PAO1F expressing pMG078 (*cdrA*-GFP) showing *cdrA*^{on} bacteria from 4 - 24 h post-infection.
1067 Cells were infected with bacteria at a MOI of 10 and incubated for 3 h. At 3 h antibiotic containing
1068 media were added to kill extracellular bacteria only (amikacin, 200 µg/mL) or extracellular and
1069 intracellular bacteria (amikacin, 200 µg/mL and ofloxacin, 0.25 - 4 µg/mL [1-16X MIC]). Cells
1070 were imaged at 1 h intervals for 20 h. Blue = Hoechst staining of nuclei (added during incubation
1071 period), Red = Propidium Iodide staining (added at 3 h to stain dead host cells), Green = bacteria
1072 expressing GFP.

1073

1074 **Supplemental Video S3.** Time-lapse imaging of human corneal epithelial cells infected with
1075 PAO1F Δ *exsA* expressing pGFP_{arabinose} showing total intracellular vacuolar bacteria from 4 - 24 h
1076 post-infection. Cells were infected with bacteria at a MOI 10 and incubated for 3 h. At 3 h,
1077 antibiotic containing media was added to kill extracellular bacteria only (amikacin, 200 µg/mL) or
1078 extracellular and intracellular bacteria (amikacin, 200 µg/mL and ofloxacin, 0.25 - 4 µg/mL [1-
1079 16X MIC]). Cells were imaged at 1 h intervals for 20 h. Blue = Hoechst staining of nuclei (added
1080 during incubation period), Red = Propidium Iodide staining (added at 3 h to stain dead host cells),
1081 Green = bacteria expressing GFP.

1082

1083 **Supplemental Video S4.** Live confocal imaging of the cornea of a Lyz2cre+/mRosa-DTR mouse
1084 infected for 15 h with mPAO1-pMG055 (EBFP2 [blue], pseudo-colored cyan) using the corneal
1085 scarification model. Video shows intracellular cytosolic bacteria that have occupied membrane

1086 blebs and distinct blue puncta suggesting bacteria located in vacuoles. Horizontal projection of the
1087 X-Y plane to the right and Y-Z plane in the lower panel.

1088

1089 **Supplemental Video S5.** Live confocal imaging of the cornea of a Lyz2cre+/mRosa-DTR mouse
1090 infected for 15 h with mPAO1-pMG055 (EBFP2 [blue], pseudo-colored cyan) using the corneal
1091 scarification model. Video shows an inset of cytosolic bacteria that have occupied membrane blebs
1092 some demonstrating rapid swimming motility.

1093

1094 **Supplemental Video S6.** Live confocal imaging of the cornea of a Lyz2cre+/mRosa-DTR mouse
1095 infected for 15 h with mPAO1-pMG055 (EBFP2 [blue], pseudo-colored cyan) using the corneal
1096 scarification model. Video shows an inset of blue puncta indicative of bacteria within vacuoles.

1097

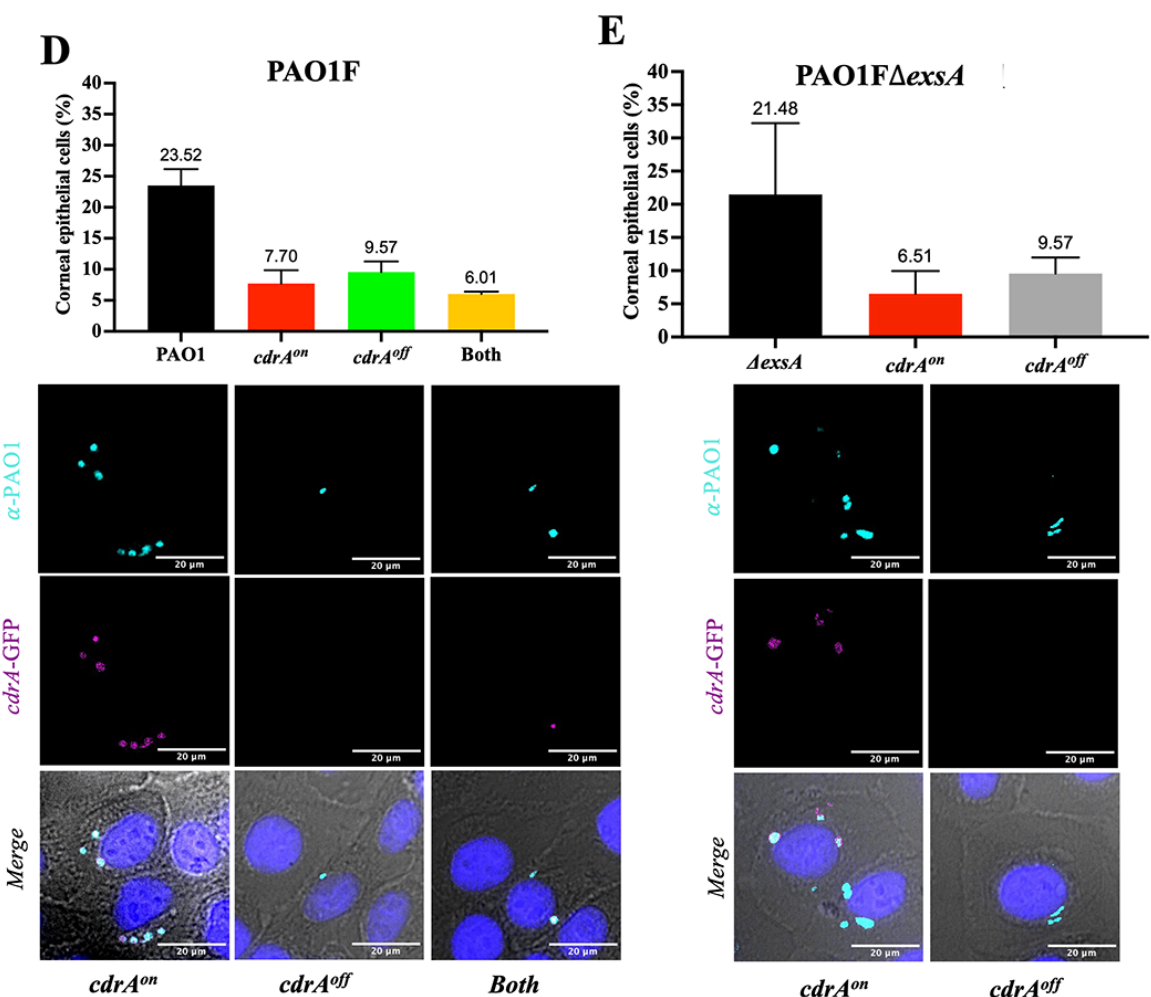
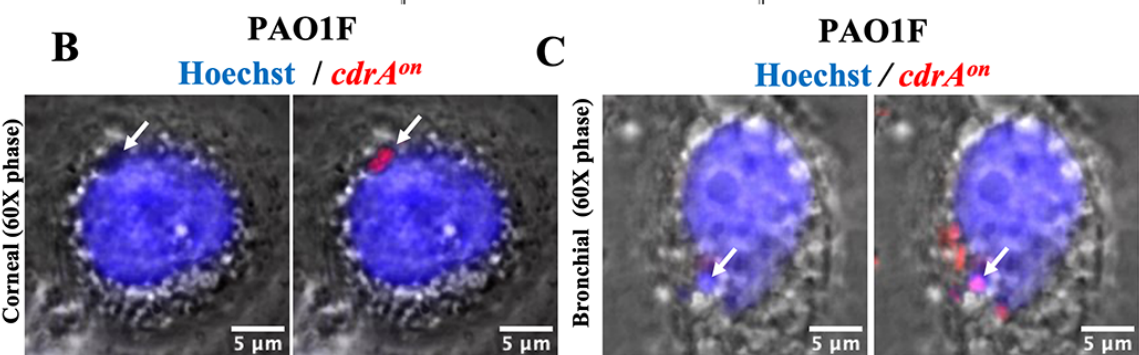
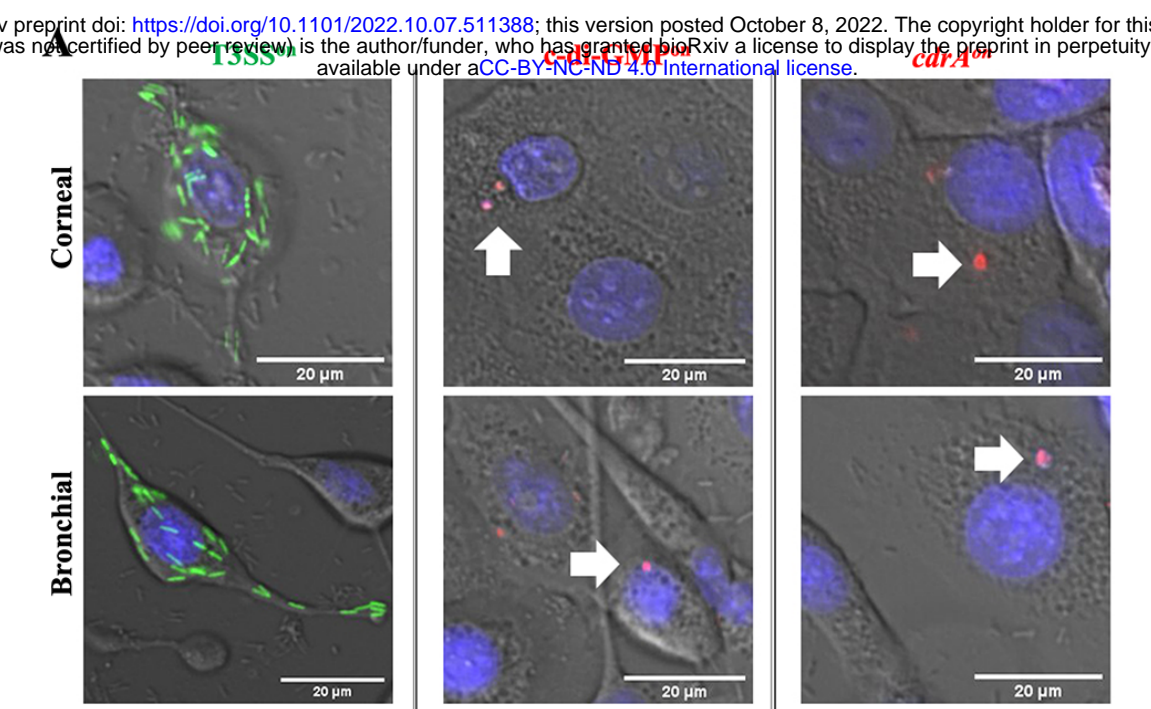
1098 **Animal Statement.** All procedures involving animals were carried out in accordance with the
1099 standards established by the Association for the Research in Vision and Ophthalmology, under a
1100 protocol AUP-2019-06-12322 approved by the Animal Care and Use Committee, University of
1101 California Berkeley, an AAALAC accredited institution. This protocol adheres to PHS policy on
1102 the humane care and use of laboratory animals, and the guide for the care and use of laboratory
1103 animals.

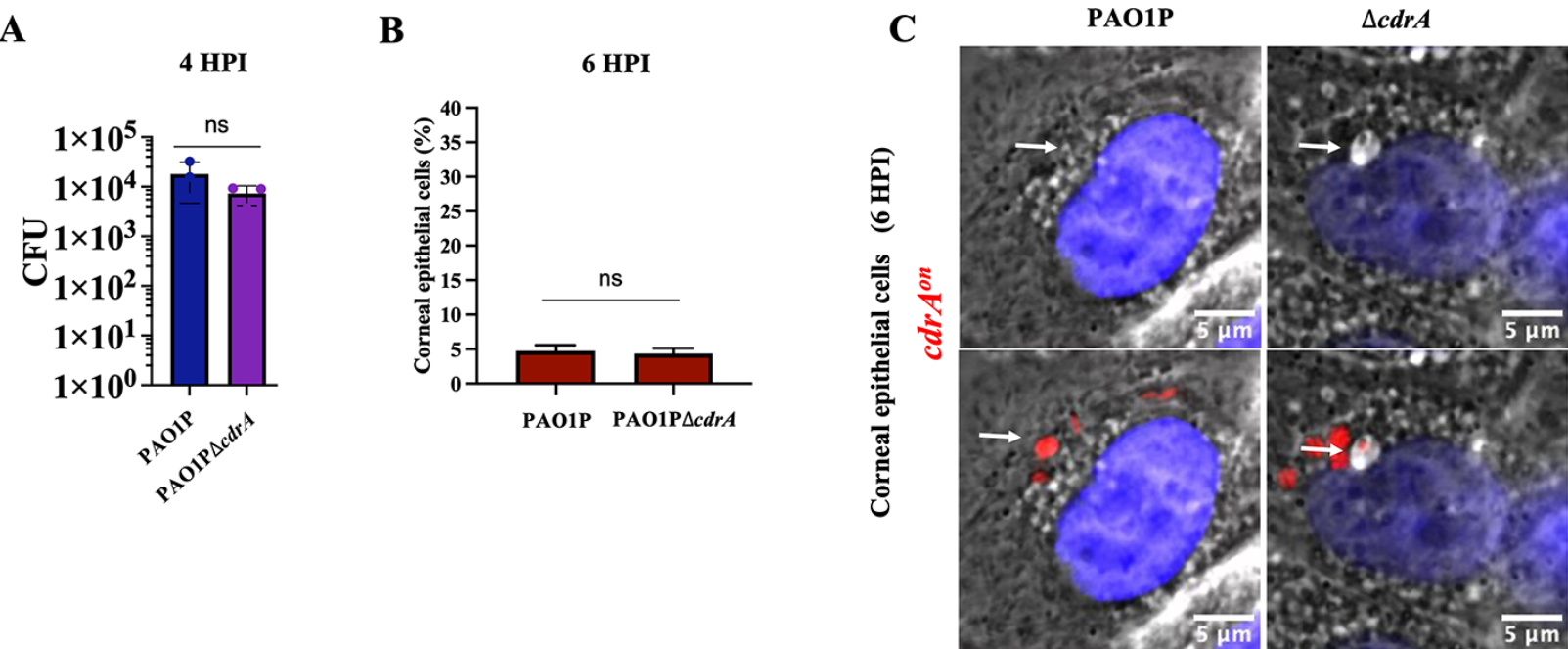
Table 1. *P. aeruginosa* strains, mutants and plasmids used in this study

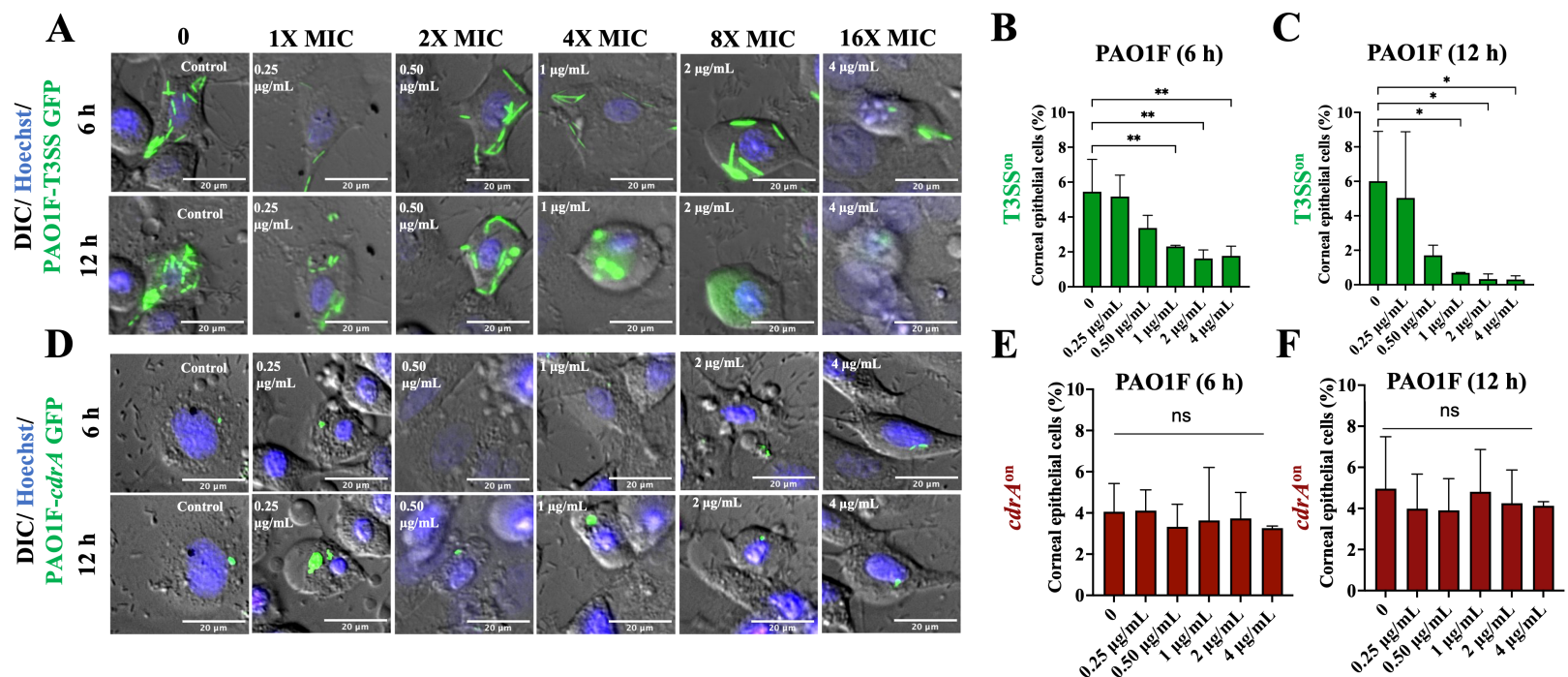
Name		Description	Source
Strain or Mutant			
PAO1F		Wild-type	Dr. Alain Filloux
PAO1FD exsA		<i>exsA</i> mutant	Dr. Alain Filloux
PAO1P		Wild-type	Dr. Matthew Parsek (34)
PAO1P cdrA		<i>cdrA</i> mutant	Dr. Matthew Parsek (34)
PAO1P EPS		<i>psl</i> , <i>pel</i> , <i>algD</i> mutant	Dr. Matthew Parsek (32)
PAO1P EPS cdrA		<i>psl</i> , <i>pel</i> , <i>algD</i> , <i>cdrA</i> mutant	Dr. Matthew Parsek (32)
mPAO1		Wild-type PAO1	<i>Pseudomonas</i> transposon library (72)
Plasmid			
pMG078	<i>pBBR1 oriV</i>	<i>cdrA</i> -GFP	This study
pFY4535		c-di-GMP Turbo-RFP reporter	Dr. Fitnat Yildiz (39. 40)
pJNE05	<i>Plasmid:</i> <i>pJN105</i> , <i>ori:</i> <i>pBBR1oriV</i>	T3SS-GFP expression vector (pJNE05:: <i>exoS</i> -GFP)	Dr. Timothy Yahr (73)
pBAD-GFP (pGFP _{arabinose})	<i>Plasmid:</i> <i>pJN105</i> , <i>ori:</i> <i>pBBR1oriV</i>	Arabinose-inducible GFP (pTJ1::araGFP)	This study
pMG055	<i>Plasmid:</i> <i>pTJ1</i> , <i>ori:</i> <i>oriT</i>	Constitutive blue fluorescent protein (EBFP2)	This study

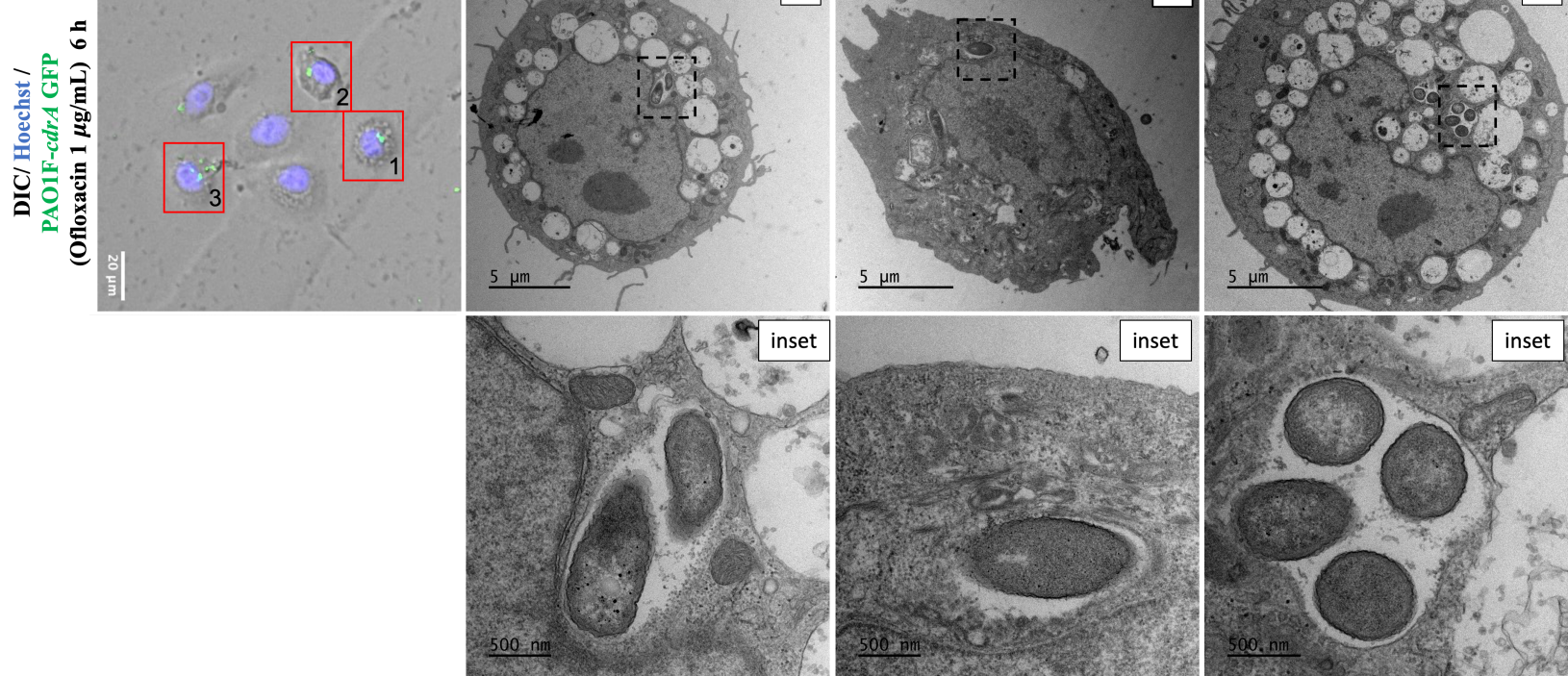
Table 2. Primers used in this study

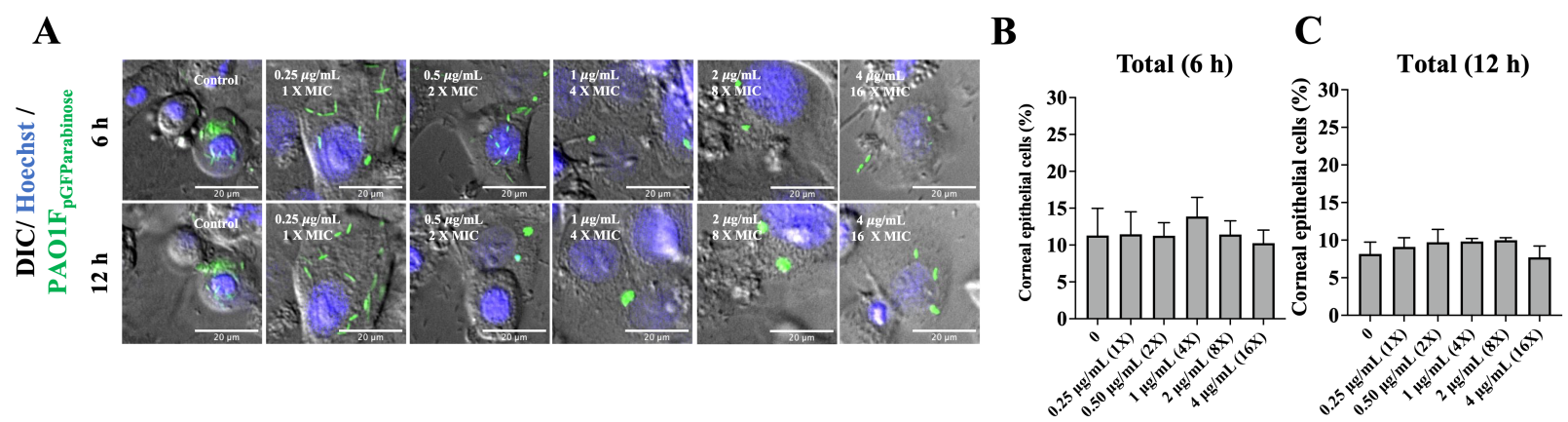
ID	Primer Name	Sequence (5' - 3')	Restriction Site	Expected Size
P019	pJNE05_part1.1a	ACCTTCGGGAGCGCCTGA		3106bp
P020	pJNE05_part1.1b	agtactattgaacgcgtGAATTCTGGCT TATTCCCTAAC		
P021	pJNE05_part2.1a	ttaggaaataagccgaattcacgcgttaatagt actAAGCTTCCGATCCCCAATT CC		3486bp
P022	pJNE05_part2.1b	cttcaggcgctcccgaaaggCTCGGGCC GTCTCTTGGG		
P032	cdrA.1a	cactaagtactCATTGTCGGTTTT TGACGG		
P033	cdrA.1b	cactaacgcgtCGCACGTCAGTTTT CCAGCA		
P010	ptac-dTomato.1a	TTATAggcgccctgcaggtcgtaatca ctgc	Ascl site	419bp plus dTomato ~1kb
P011	ptac-dTomato.1b	TATTAgcggccgcctctctcatcccaa aac	NotI site	
P014	T0T1- terminators.1a	atgagagaaggcgccAGCTTAAT TAGCTGAGCTTGG	Ascl site mid-primer	300bp
P015	T0T1- terminators.1b	cctattctagaacttagtgcGGCGGATT TGTCTACTC		
P027	ebfp2.1a	cactaggatccAATGGTGAGCAAG GGCGAGG	BamHI site	746bp
P029	ebfp2.2b	CACATAAGCTTCTACTTGTAA CAGCTCGTCCATGCC	HindIII site	
P012	pMG035- gibson.1a	taccggggccccccctcgaggcgacTGCA GGTCGTAAATCACTG	Sall site mid-primer	1075bp
P013	pMG035- gibson.1b	ttaagctggcgccCTTCTCTCATC CGCCAAAAC	Ascl site mid-primer	

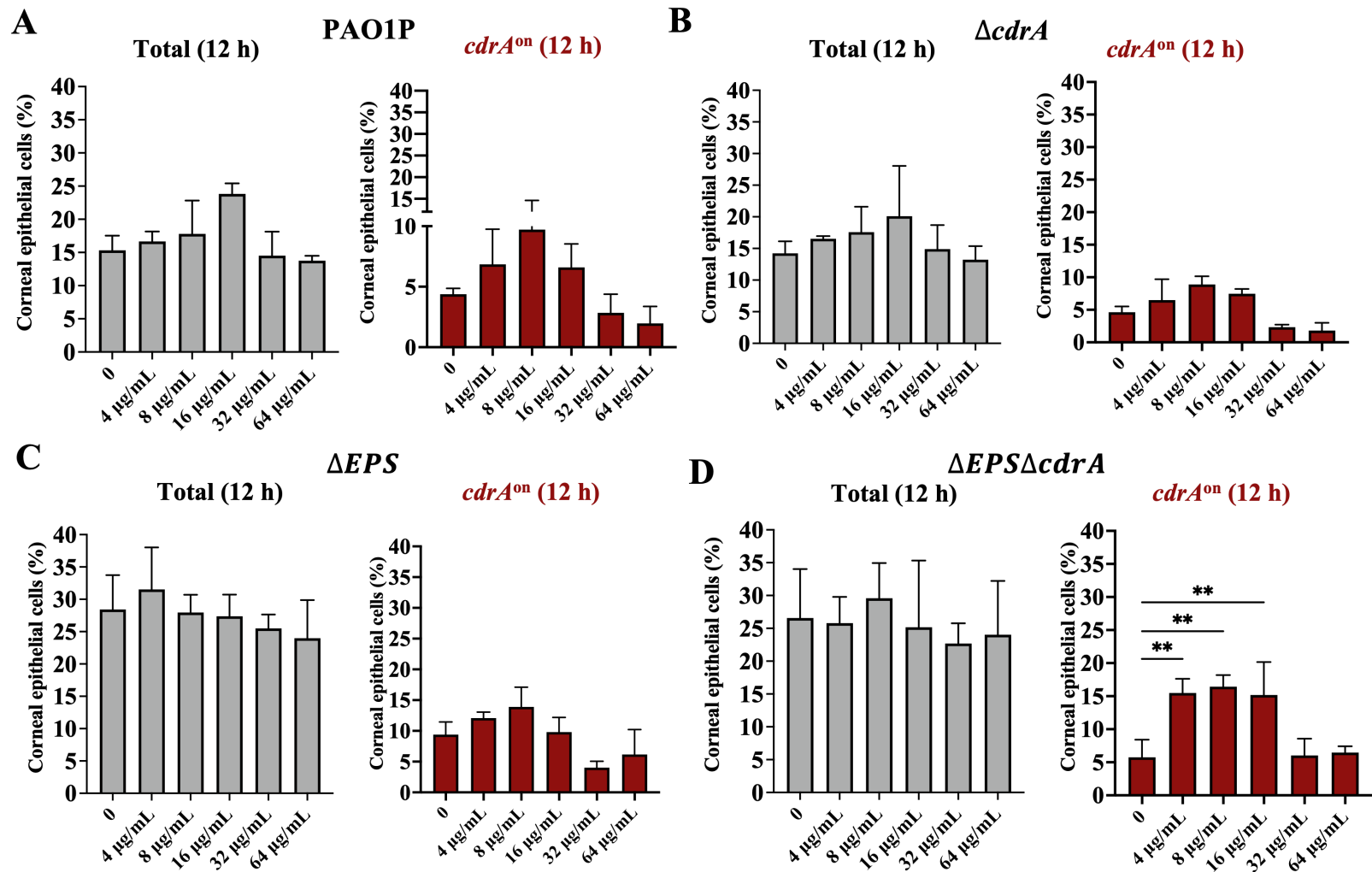


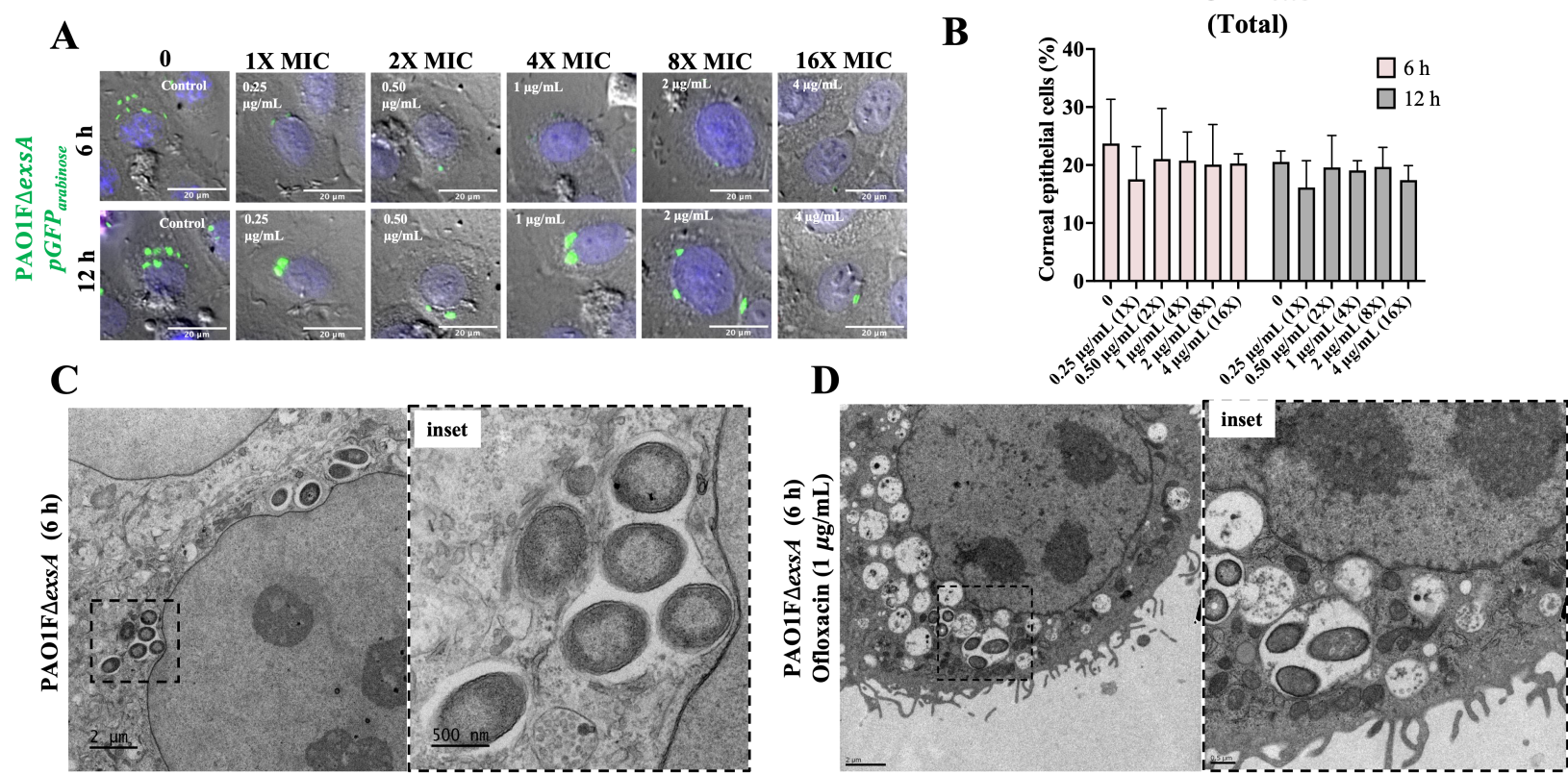




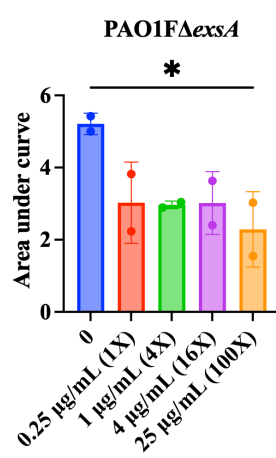
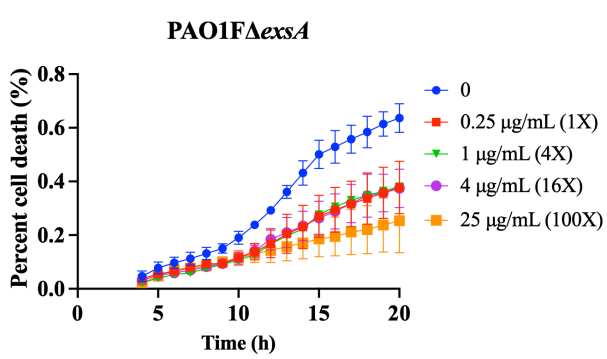




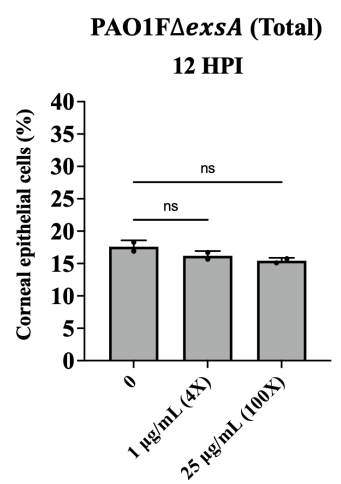




A



B



Lyz2^{cre}/mRosa DTR mice
PAO1 (15 HPI)

